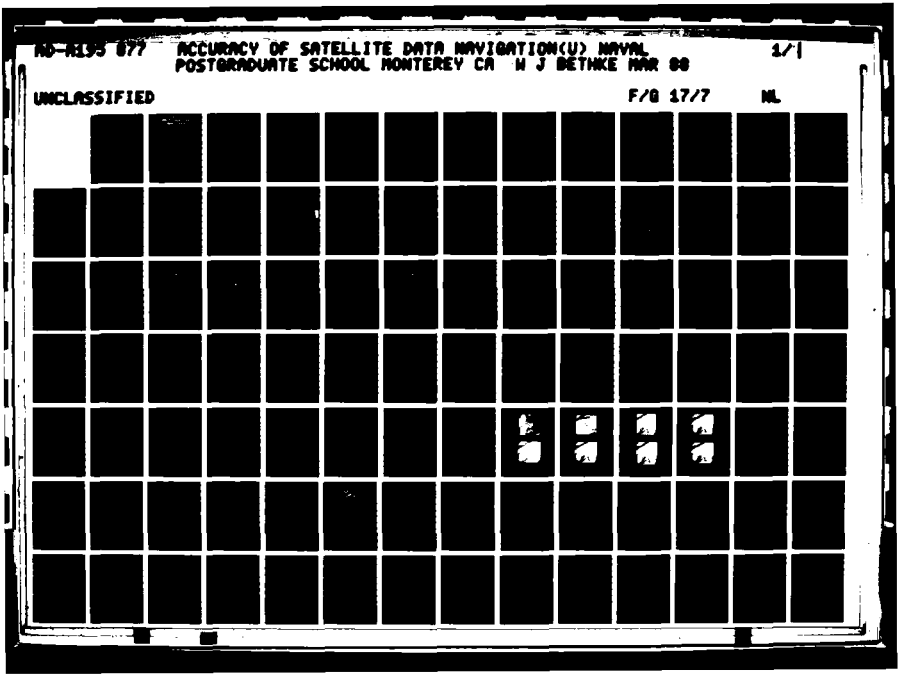
AD-A195 877
ACCURACY OF SATELLITE DATA NAVIGATION(U) NAVAL POSTGRADUATE SCHOOL MONTEREY CA W J BETHKE MAR 88
1/1
UNCLASSIFIED
F/G 17/7
NL

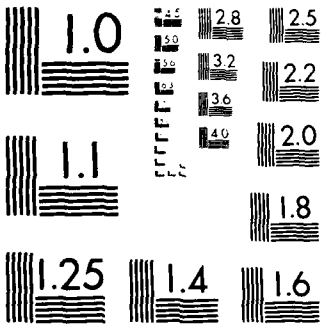

NAVAL POSTGRADUATE SCHOOL
Monterey, California

THESIS

ACCURACY OF SATELLITE DATA NAVIGATION

by

William J. Bethke

March 1988

Thesis Advisor: C. H. Wash
Co-advisor P. A. Durkee

REPORT DOCUMENTATION PAGE

1a REPORT SECURITY CLASSIFICATION UNCLASSIFIED	1b RESTRICTIVE MARKINGS
2a SECURITY CLASSIFICATION AUTHORITY	3 DISTRIBUTION/AVAILABILITY OF REPORT Approved for public release; distribution is unlimited
2b DECLASSIFICATION/DOWNGRADING SCHEDULE	
4 PERFORMING ORGANIZATION REPORT NUMBER(S)	5 MONITORING ORGANIZATION REPORT NUMBER(S)
6a NAME OF PERFORMING ORGANIZATION Naval Postgraduate School 6b OFFICE SYMBOL (If applicable) Code 63	7a NAME OF MONITORING ORGANIZATION Naval Postgraduate School
6c ADDRESS (City, State, and ZIP Code) Monterey, California 93943-5000	7b ADDRESS (City, State, and ZIP Code) Monterey, California 93943-5000
8a NAME OF FUNDING/SPONSORING ORGANIZATION 8b OFFICE SYMBOL (If applicable)	9 PROCUREMENT INSTRUMENT IDENTIFICATION NUMBER
8c ADDRESS (City, State, and ZIP Code)	10 SOURCE OF FUNDING NUMBERS PROGRAM ELEMENT NO / PROJECT NO / TASK NO / WORK UNIT ACCESSION NO

11 TITLE (Include Security Classification)
ACCURACY OF SATELLITE DATA NAVIGATION

12 PERSONAL AUTHOR(S)
Bethke, William J.

13a TYPE OF REPORT	13b TIME COVERED	14 DATE OF REPORT (Year, Month, Day)	15 PAGE COUNT
Master's Thesis	FROM _____ TO _____	1988, March	98

16 SUPPLEMENTARY NOTATION
The views expressed in this thesis are those of the author and do not reflect the official policy or position of the Department of Defense or the U.S. Government.

17 COSATI CODES			18 SUBJECT TERMS (Continue on reverse if necessary and identify by block number)
FIELD	GROUP	SUB-GROUP	Image Navigation; Image Registration; Satellite Orbit Modelling

19 ABSTRACT (Continue on reverse if necessary and identify by block number)
Image navigation is critical to the effective use of digital imagery for meteorological and oceanographic studies. This thesis reviews various methods used to navigate imagery to the earth and investigates the accuracy of the Naval Postgraduate School (NPS) model. An explanation of how the NPS navigation process works is included for completeness. Results from 22 separate runs of the NPS model are studied. The following points are discussed in Chapters VI and VII:

1. Abilities of user affects accuracy.
2. Apparaent upper bound for navigation landmarks.
3. Centrally oriented navigation landmarks enhance accuracy.
4. Evenly distributed navigation landmarks enhance accuracy.

The thesis concludes with observations and suggestions to stimulate further research into the effective use of the NPS image navigation system.

20 DISTRIBUTION/AVAILABILITY OF ABSTRACT ☒ UNCLASSIFIED/UNLIMITED ☐ SAME AS RPT ☐ DTIC USERS	21 ABSTRACT SECURITY CLASSIFICATION Unclassified
22a NAME OF RESPONSIBLE INDIVIDUAL Prof. C.H. Wash	22b TELEPHONE (Include Area Code) (408) 646-2295 22c OFFICE SYMBOL Code 63Wx

Approved for public release; distribution is unlimited.

Accuracy of Satellite Data Navigation
by

William J. Bethke
Captain, United States Marine Corps
B.S., University of Nebraska, 1982

Submitted in partial fulfillment of the
requirements for the degree of

MASTER OF SCIENCE IN SYSTEMS TECHNOLOGY
(SPACE SYSTEMS OPERATIONS)
from the
NAVAL POSTGRADUATE SCHOOL
March 1988

Author: William J. Bethke
William J. Bethke

Approved by:
C. H. Wash, Thesis Advisor

P. A. Durkee, Co-advisor

Rudolf Panholzer, Chairman,
Space Systems Academic Group

Gordon E. Schacher,
Dean of Science and Engineering

ABSTRACT

Image navigation is critical to the effective use of digital imagery for meteorological and oceanographic studies. This thesis reviews various methods used to navigate imagery to the earth and investigates the accuracy of the Naval Postgraduate School (NPS) model. An explanation of how the NPS navigation process works is included for completeness. Results from 22 separate runs of the NPS model are studied. The following points are discussed in Chapters VI and VII:

1. Abilities of user affects accuracy.
2. Apparent upper bound for navigation landmarks.
3. Centrally oriented navigation landmarks enhance accuracy.
4. Evenly distributed navigation landmarks enhance accuracy.

The thesis concludes with observations and suggestions to stimulate further research into the effective use of the NPS image navigation system.

TABLE OF CONTENTS

LIST OF TABLES

LIST OF FIGURES

I. INTRODUCTION

Navigation, as it applies to the satellite image analysis community, involves the process of registering remotely sensed satellite digital imagery to its corresponding earth features. Once accomplished, a one to one correspondence is established between points in the digital imagery and points on the earth. This association, also called image registration, allows the application of positional references such as coastlines and latitude and longitude grid lines. These references facilitate the location of specific meteorological and oceanographic phenomena. The ability to register such features is critical to the effective use of the digital imagery.

Registration can be accomplished using a variety of methods. Some of the commonly used techniques are discussed in Chapter II. The process used by the Naval Postgraduate School (NPS) locates the satellite's position at the time the imagery was taken. The accomplishment of this allows the calculation of the sub-satellite and nodal points with respect to the imagery. The knowledge of the sub-satellite and nodal point location is used to determine the latitude and longitude of selected landmarks which ultimately permits registration of the imagery to the earth.

Accuracy of the navigation process is determined by the ability of algorithms, which represent the imaging satellite's motion, to correctly model all of the forces acting on the satellite. It is also dependent on systematic errors and inaccuracies in both landmark selection on the satellite imagery and determining landmark geographic positions.

Determination of the accuracy of the navigation process and the effects that various landmark selection schemes have on the accuracy, will increase the confidence placed on the location of an environmental feature. If grids applied to the imagery are not accurate to within a certain tolerance, then the feature(s) can only be located to within the inherent accuracy of the navigation process. The accuracy of the model used at NPS has not been rigorously tested.

The goal of this thesis is to investigate the accuracy of the NPS model and provide some insight into the model results, given various landmark selection schemes. The thrust of this thesis is divided into two parts; the first part presents techniques that are used to model satellite orbital characteristics. The discussions explore the perturbative forces acting on the National Oceanic and Atmospheric Administration (NOAA) polar orbiter and the extent that the navigation program used at NPS models these forces. The second part evaluates the accuracy of the navigation program by developing a landmark selection

strategy and applying it to the program. An estimate of the accuracy of the navigation process is obtained by running the program using landmarks selected in several different patterns and measuring the differences between the calculated values of latitude and longitude and the geographic latitude and longitude of the landmarks. Improvements are suggested for further investigation. The discussions that follow assume the reader has a rudimentary understanding of the terminology used in conjunction with environmental satellite operations. Appendix A includes a glossary of relevant terms.

II. BACKGROUND

Accurate registration of satellite imagery is critical for determining the position of environmental phenomena on the earth. Various methods have been developed to orient a satellite image to the earth. The methods can be broadly classified into two categories: (1) physical manipulation of the imagery using overlays; and (2) computer assisted registration of the imagery (Clark, et al., 1981:224).

A. PHYSICAL MANIPULATION OF IMAGERY

The physical manipulation of imagery and reference baselines to orient the imagery to the earth generally involves the use of overlays that are representative of the area on the image. The overlays consist of latitude and longitude grids and geographical features such as coastlines and landmarks. The imagery is registered to the earth by placing an overlay on top of the imagery and physically rotating the overlay until reference landmarks on the imagery match landmarks on the overlay. This method does not produce very accurate mappings of the imagery. However, it is a simple method which can be applied when accuracy is not critical. Since the use of overlays is relatively straightforward, there has not been a large amount of documentation discussing the techniques involved. The discussion of image registration using overlays is generally

found in reports on more accurate computerized methods of image registration (Clark, et al., 1981:229). It is often cited as an example of a less accurate method that has been used in the past.

B. COMPUTER ASSISTED REGISTRATION

The second category of image registration involves the use of computers to establish mathematical relationships between the location of the imaging satellite and the locations of landmarks picked from the imagery whose geographical locations on the earth are known. The origin of the digital imagery being navigated determines the processes that will be used to register it. Imagery can be obtained in two forms: direct downlink from the satellite (real time data) and archived on computer compatible tapes (CCTs). If the imagery is received in CCT format, the source of the data becomes important since different agencies use different methods to process and append navigational information to the raw digital data as it is transformed into CCTs.

In either case, the first step in the navigational process is the accurate determination of the position of the satellite with respect to the digital imagery.

1. Real Time Imagery

Digital imagery and satellite data obtained in real time contain accurate positioning information for the

satellite and, therefore, do not need complicated algorithms to determine the satellite's position.

An example of a real time method of registering imagery is presented by Brush (1985). Brush develops a methodology to navigate NOAA-7 satellite imagery. The process begins with the selection of latitude and longitude pairs which define a reference set. These reference pairs "may represent lines of equal latitude/longitude or...coast-lines." (Brush, 1985:877) X and y values are then calculated for the reference set; the x value is equal to the distance away from the satellite's ground track, and the y value is the distance along the track measured from the ascending node. These values give the location of a landmark as a function of the satellite's position (ground track). Knowing the track of the satellite in the image, it is then a simple process to determine where latitude and longitude grids should lie in terms of x and y. The program uses a finite number of points for grid generation and interpolates between them to fully determine the grid lines both East/West and North/South. Since this is all done using real time data there is no need to solve for the satellite's position using Kepler's equation or using other well-known methods. The process is simple and easy to follow and the results are printed out on a facsimile machine for real-time data interpretation. Brush (1985) indicates that the image registration technique presented in

his paper is accurate. However, a numerical measure of the accuracy was not disclosed.

A rather unique method of image registration using real-time imagery obtained from Defense Meteorological Satellites is given by Cherne (1974). The methodology described determines the location of a finite set of selected landmarks with respect to scan planes, then uses double linear interpolation to find the positions of landmarks that are located in-between the original landmarks. The algorithm begins with five rotation matrices that translate an imaginary satellite from an equatorial orbit to the position of the satellite at the time the imagery was taken. The routine then determines the two scan planes bordering the selected landmark, calculates the scan line that views the landmark, and finally calculates the sample within the line that observes the landmark. This results in the line and column (pixel) on the imagery that represents the landmark. The mapping of the imagery to the earth is completed after all of the landmarks have been registered. The final output is an array oriented to a particular map projection. The calculations are performed in the following steps:

1. Compute the direction numbers that describe the vector pointing in the direction of movement of the satellite, perpendicular to the scan line.
2. Compute the source (scanner) location.

3. Obtain scan planes corresponding to the scan lines used as bench lines, using the results of 1 and 2 above.

4. Calculate the X,Y,Z location on the earth's surface (geocentric equatorial reference system) of the landmarks, given their latitude and longitude.

5. Calculate which two scan planes the landmark falls between.

6. Determine source location, scan line, time of observation and solar locations of the landmark given the ratio of the perpendicular distances between the landmark and the two bracketing scan planes.

7. Compute the angle from nadir to determine which sample of the interpolated line observed the landmark.

Given the scan line and the sample within the scan line that observes the landmark, the pixel (picture element) that represents the landmark is determined.

The preceding method was being used by the Air Force Global Weather Central at Offutt Air Force Base at the time of writing of the Cherne article (1974). The accuracy of the procedure was not specified beyond saying that the system produced accurate and timely results. Timeliness was demonstrated: "On a Univac 1110 computer, a strip on a polar stereographic projection from pole to equator which considered 2277 map bench points (33 x 69) is processed in 2 seconds wall time." (Cherne, 1974:51) The strength of the Cherne method lies in its optimal use of data processing equipment, its timeliness, and its ability to maximize software stability and programmer control (Cherne, 1974:iv).

2. Archived Imagery

Users who are unable to obtain real time imagery must use archived digital data available on magnetic tapes. The format and contents of the image bearing tapes depends upon the originating agency. Some tapes have positional information appended to them, others do not.

a. CCTs Containing Position Information

Computer compatible tapes (CCTs) distributed by the National Environmental Satellite, Data, and Information Service (NESDIS) contain positioning information. The latitude and longitude of 51 equally spaced points on 25 scan lines of the Advanced Very High Resolution Radiometer (AVHRR) scanner are calculated by the Grid and Earth Location System (GELDS) (Kidwell, 1986:3.9). The locations of the points are determined by algorithms that use both the satellite's ephemeris data and the operational characteristics of the AVHRR scanner as input. The ephemeris data, combined with the operational attributes of the NOAA polar orbiter, allow the determination of the position of the satellite with respect to the earth. Once the position of the satellite is known, the locations (latitude and longitude) of individual points along each scan line are calculated using a model of the sensor-satellite geometry to determine where the sensor is pointing as a function of time, given the location of the satellite at that particular time. This positional information is calculated before any

digital imagery is received and is wholly dependent on the geometrical relationships between NOAA polar satellites, the scanners carried on board, and the satellite's position relative to the earth. The output of the GELDS is stored on tapes until receipt of satellite imagery that corresponds to the tapes. When the appropriate imagery is received, the positional information is appended to it. Systems using tapes containing positional information can avoid the large amount of work that is associated with generating the information since it is already appended to the tapes. Clark and La Violette (1981) describe a method of registering TIROS-N imagery using the geographical coordinates contained in CCTs obtained from NESDIS. The accuracy of the navigation process is stated as follows: "for 32 landmark locations, the mean positioning error was 3.7 km with a standard deviation of 1.7 km." (Clark, 1981:230) The advantage of using CCTs that contain position information is that the positions of Ground Control Points (GCPs) within the imagery are already included on the CCTs, and the use of this information eliminates the necessity to calculate the position of GCPs during image registration.

b. CCTs Without Position Information

Many other agencies, such as the National Aeronautics and Space Administration (NASA), the Scripps Institution of Oceanography, and ground stations operated by

the Department of Interior, which archive satellite imagery, do not append navigational information to their tapes. These tapes include those used by NPS. The tapes used at NPS do not contain any positioning information other than the satellite's ephemeris data at some specific time. This time generally does not correspond to the time that the image was taken and, as a consequence, the satellite's position within the imagery must be updated. Calculation of the satellite's position entails solving Kepler's equation. The calculations associated with solving Kepler's equation are discussed in Chapter III.

C. COMMENTS

The basic procedure of locating the imaging satellite within the image plane and determining the locations of landmarks both in the image and on the surface of the earth is common to all but the overlay method of image navigation. The methods briefly discussed above are a representative sample of routines currently in use. For a more detailed study, the interested reader is invited to review the publications listed in the bibliography of this thesis.

The determination of the imaging satellite's position in reference to the image plane is the first, and most difficult, procedure in registering the satellite imagery. Accurate modeling of the NOAA polar orbiting satellite's orbital characteristics is mandatory if the satellite is to be precisely located within the image plane. Chapter III

discussed the issue of modeling the imaging satellite's orbital behavior.

III. DETERMINING SATELLITE POSITION

A. DEFINITION AND IMPORTANCE

Determining the position a satellite involves locating the satellite in its orbital plane given known characteristics of the satellite's motion.

The importance of properly locating a satellite cannot be overemphasized. Without a knowledge of where the satellite is in reference to the image plane, the navigation of the imagery would be virtually impossible. Determining the location of a satellite is difficult, involving solutions to complex algorithms and trigonometric relationships. However, the process is eased as more information is made available to the user.

The most commonly used method of locating a satellite in its orbit involves the solution to Kepler's equation. Kepler's equation relates the satellite's mean anomaly (M) to its eccentric anomaly (E) and orbit eccentricity (e), ($M = E - e\sin E$). The mean anomaly (M) is "the angle through which an object would move at the uniform average speed n [mean motion] in a time $t-t_0$, measured from perifocus [perigee]." (Baker, et al., 1967:388) The mean anomaly is dependent on the mean motion (n) of the satellite as shown:

$$M = n(t-T) = M_0 + n(t-t_0) \qquad (3.1)$$

where M_0 is the value of M at the specified epoch time t_0 and t represents a later time (Baker, et al., 1967:11). The orbital position of the satellite, as a function of time, is determined by relating the two equations for M. The eccentric anomaly (E) is the angle measured from the major axis (A) to a line extended from the center of the ellipse to a point on the circumscribing circle whose position is determined by drawing a line from the satellite's position, perpendicular to the major axis, up to the circumscribing circle (Figure 1).

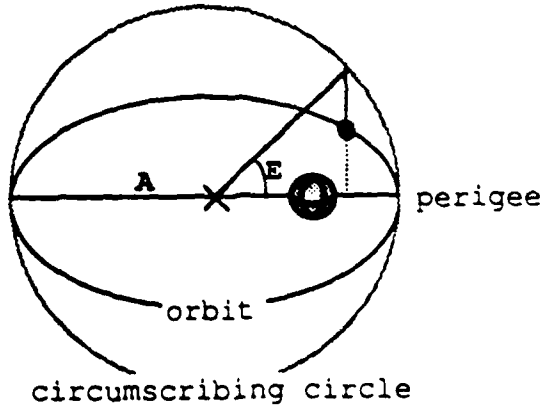

Figure 1. Eccentric Anomaly

B. PERTURBING FORCES

An earth satellite experiences various forces which cause its orbital motion to deviate from the motion predicted by a simple Keplerian two body model. Depending on the characteristics of the satellite's orbit, the complexity of an orbital model will range from simple two-body Keplerian descriptions of the orbital elements to complex Bessel series representations of the perturbations to the satellite's orbit.

Orbital elements such as orbital height and eccentricity, and physical characteristics such as the surface area of the satellite, determine the forces that must be considered. For example, modeling satellites which orbit the earth at low altitudes requires the consideration of atmospheric drag forces while these forces may be ignored for satellites in higher orbits. Similarly, satellites in highly elliptical orbits that come within a few hundred miles of the earth at perigee are greatly affected by atmospheric drag while geostationary satellites are not. Thus, the complexity of the algorithms which predict the location of a satellite is determined by the type of satellite orbit. A balance is sought between complexity of the algorithm, necessity of modeling a force, and acceptable accuracy in modeling the satellite motion. In order to make these assessments, one must become familiar with the forces

involved. The most significant perturbative forces and their descriptions are (El'yasberg, 1967):

1. Asymmetrical gravitational force--A gravitational force that includes the increase in the gravitational force of the earth caused by the oblateness of the earth. The asymmetrical gravitational force causes precession of the orbit (line of the nodes) and is the most significant perturbative force.

2. Atmospheric drag--A force acting opposite to the direction of movement of a satellite which decreases the energy of the satellite causing its orbit to decay. It is the result of a satellite moving through a viscous atmosphere. Predicting the effects of atmospheric drag involves uncertainties in atmospheric density due to solar influences.

3. Radiation pressure--A force caused by the impingement of solar radiation on the surface of the satellite.

4. Atmospheric lift--Forces produced by the differences in pressure on two sides of a body moving through the viscous atmosphere.

5. Thrust--Involves perturbations caused when the satellite uses its thrusters to move and the necessary damping out of the resultant fluctuations.

6. Force of attraction of other bodies--Gravitational force of attraction between other celestial bodies, e.g., the sun, the moon, and the satellite.

C. SATELLITE MODELS

The most rudimentary model of satellite motion is the simple two body problem utilizing Keplerian equations which ignore all of the above forces. In this model the earth is considered to be a perfect sphere or a gravitational point mass. Such a model is not sophisticated enough to accurately represent the environmental satellites under consideration.

The more complex models consider the oblateness of the earth, its effect on the gravitational force, and the subsequent effect on the satellite's orbit. Perturbations caused by the oblateness of the earth are the most significant factors which cause deviations in the satellite's motion. Modeling the perturbations produces reasonably accurate position calculations that are precise enough for many applications.

The most complex models consider some or all of the other perturbative forces. Adding each of the other perturbative forces may or may not be useful depending on the type of satellite orbit under consideration. The most important perturbative force acting on NOAA and Defense Meteorological Satellite Program (DMSP) satellites is the asymmetrical gravitational force. This force causes changes in the mean motion of the satellite which affects the ability to locate the satellites in their orbits. To account for these effects, the navigation model used at NPS considers the oblateness of the earth (thus the asymmetrical gravitational force). The other perturbative forces are considered insignificant for a variety of reasons. Atmospheric drag is considered insignificant because the NOAA/DMSP satellites are at an altitude where atmospheric drag effects are negligible (850 Km). Radiation pressure, atmospheric lift, and the rest of the perturbing forces are compensated for by updating the ephemeris data base at least

every two weeks. Any changes in the orbital characteristics caused by these perturbative forces over a two week period are considered negligible. For completeness, however, a decay rate coefficient is included in the NPS model to alleviate any effects of perturbative forces not directly modeled. The decay coefficient represents the anomalous motion of the satellite that is not compensated for by modelling the earth's oblateness. The decay rate is based on radar fixes and equations used at the North American Air Defense Command (NORAD) to determine satellite position.

D. GENERALIZED SATELLITE POSITIONING TECHNIQUE

There are a variety of techniques which have been used to determine the position of a satellite given its ephemeris data. The method used depends, to a large degree, on the type of orbit that the satellite is in and also on the form and content of the ephemeris data. Smith (1980) discusses a generalized technique for transforming the position of a meteorological satellite from a seven element classical coordinate system to a rotating earth coordinate system. The technique developed by Smith (1980) is summarized for the necessary background understanding of the processes involved in determining the position of a satellite.

1. Classical Elements

The seven classical elements describing a satellite's position are (Smith, 1980:58):

1. Epoch Time (t_0): The Julian day and Greenwich Mean Time (GMT) for which the following set of elements are defined.

2. Semi-major Axis (a): One half of the distance between perigee and apogee.

3. Eccentricity (e): The degree that the orbit varies from being circular (ellipticity).

4. Inclination (i): The angle between the plane of the satellite's orbit and the equatorial plane of the earth.

5. Mean Anomaly (M_0): An angle in the orbital plane with respect to the center of a circle circumscribed around the given orbit, from perigee to the satellite's position. The circle used is generally described as a mean circular orbit having a period equivalent to the anomalistic period of the satellite. (The anomalistic period is described in Appendix A.)

6. Right Ascension of Ascending Node (Ω_0): Angle in the equatorial plane between the vernal equinox (reference meridian) and the northward equator crossing (ascending node).

7. Argument of Perigee (ω_0): Angle in the orbital plane from the ascending node to perigee.

These elements are all that are needed to represent the position of a satellite in the 7-element classical coordinate system (Figure 2). For many applications, however, the position of the satellite must be known with respect to a rotating earth coordinate system. In fact, the determination of a satellite's sub-satellite point requires this. The next section discusses a method of translating the position of a satellite in the 7-element classical coordinate system to the rotating earth coordinate system. Unless otherwise stated, the equations used throughout the rest of this chapter have been extracted from Smith (1980).

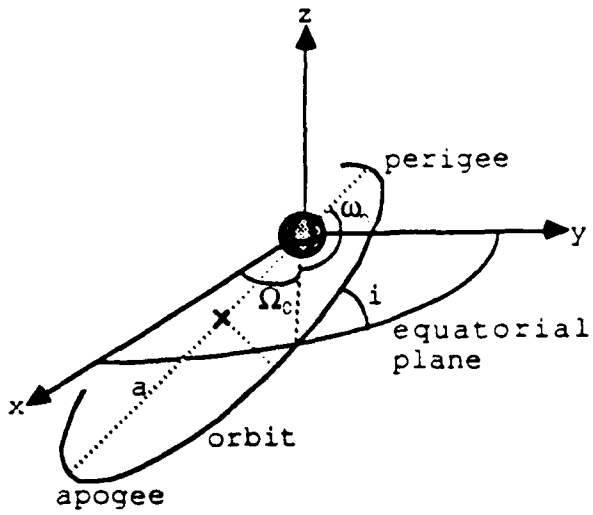

Figure 2. 7-Element Classical Coordinate System (following Smith, 1980)

2. Satellite Location Process

The satellite location process, outlined below, assumes a point mass earth and a satellite represented as a mass-less point subject only to the force of gravity. This ensures that all of the elements are constant (two body Keplerian problem).

a. Perifocal Coordinate System

The first step is to convert from the classical elements to perifocal coordinates. The perifocal coordinate system is one that has the orbital plane of the satellite as its fundamental plane. Because of this, it is the easiest coordinate system to translate to from the classical elements. The perifocal coordinate system is defined by

unit vectors PQW. Figure 3 illustrates the relationship between the unit vectors. These vectors point towards perigee (P), 90 degrees from perigee in the direction of the satellite's motion (Q)(assuming a direct orbit), and orthogonally to the first two vectors (W), respectively.

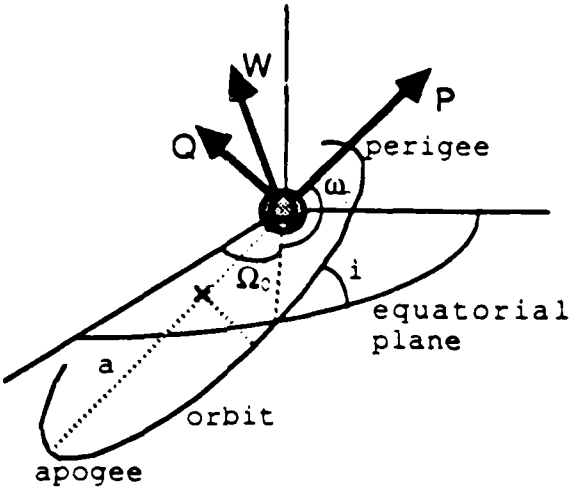

Figure 3. Perifocal Coordinate System
(following Smith, 1980)

One of the benefits of using this system is that the component of the satellite's position in the W direction is always zero; the result of the satellite's orbital plane always being in the P,Q plane. The components of the satellite's position in the P and Q direction can be calculated from:

$$x_\omega = a(\cos E - e) \qquad (3.2)$$

$$y_{\omega} = a(\sin E)\sqrt{(1 - e^2)} \tag{3.3}$$

where E is the eccentric anomaly (Figure 1). The eccentric anomaly can be approximated with sufficient precision by the expansion:

$$\begin{aligned} E = M &+ e \sin(M) + e^2 \sin(M) \cos(M) + e^3(\sin(M) \\ &- 3/2 \sin^3(M)) + e^4(\sin(M) \cos(M) \\ &- 8/3 \sin^3(M) \cos(M)) + e^5(\sin(M) \\ &- 17/3 \sin^3(M) + 125/24 \sin^5(M)) \end{aligned} \tag{3.4}$$

where M is the mean anomaly at a specified time t (i.e., not necessarily M_0). A general formula for M may be derived by:

$$M = n(t - T) \tag{3.5}$$

where t is the specified time and T is the time of perifocal passage, and can be computed from:

$$T = t_0 - M_0/n \ . \tag{3.6}$$

The mean motion constant, n, can be determined from the following relationships:

$$n = \sqrt{((m_e + m_2)/m_e)} \times \sqrt{(G \ m_e)} a^{3/2} \tag{3.7}$$

where m_e = mass of the earth, m_2 = mass of satellite, and G = the gravitational constant of the earth = 6.373×10^{-8} dyne $\times$ $cm^2 \times gm^{-2}$. Note that for the sake of computational speed, the above equation may be rewritten as:

$$E = M + e(\sin(M) + e(\sin(M)\cos(M) + e((\sin(M) - 3/2\sin^3(M)) + e((8/3\sin^3(M)\cos(M)) + e(\sin(M) - 17/3\sin^3(M) + 125/24\sin^5(M))))). \quad (3.8)$$

As mentioned above, the perifocal coordinate system is merely an easy intermediate system to get to the rotating earth coordinate system from the seven element classical coordinate system. The next step is to convert the satellite coordinates from the perifocal coordinate system to the geocentric-equatorial (IJK) coordinate system.

b. Geocentric-Equatorial Coordinate System

The IJK reference system is illustrated in Figure 4. It uses the center of the earth as the origin. The I vector points in the direction of the vernal equinox (Aries), the K vector points toward the North Pole, and the J vector is mutually orthogonal to the other two vectors (Bate, 1971:55). The components of the satellite's position in the PQR coordinate system, x_ω and y_ω, can be transformed into IJK components by the application of spherical trigonometry as follows (ω, Ω, i constant):

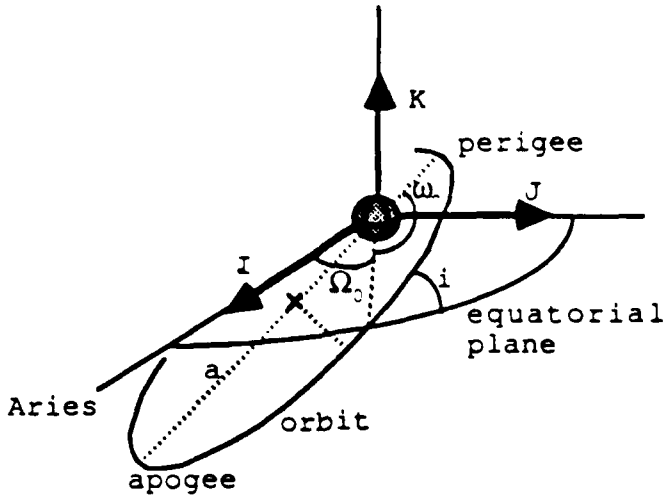

Figure 4. Geocentric-Equatorial Coordinate System (following Smith, 1980)

$$x = x_\omega(\cos(\Omega)\cos(\omega) - \sin(\Omega)\sin(\omega)\cos(i))$$
$$+ y_\omega(-\cos(\Omega)\sin(\omega) - \sin(\Omega)\cos(\omega)\cos(i))$$

$$y = x_\omega(\sin(\Omega)\cos(\omega) + \cos(\Omega)\sin(\omega)\cos(i)) \qquad (3.9)$$
$$+ y_\omega(-\sin(\Omega)\sin(\omega) + \cos(\Omega)\cos(\omega)\cos(i))$$

$$z = x_\omega(\sin(\omega)\sin(i)) + y_\omega(\cos(\omega)\sin(i)) \ .$$

The geocentric-equatorial coordinate system is a non-rotating system. To locate the position of a satellite on the rotating earth, a rotating reference frame is necessary.

c. Rotating Earth Coordinate System

The third conversion is from the geocentric-equatorial coordinate system into a rotating coordinate system and begins with determining the observer's right ascension as follows:

$$\rho = \rho_0 + d\rho/dt(t - t_0) \tag{3.10}$$

where ρ_0 is the sidereal hour angle SHA at epoch (t_0) and $d\rho/dt = 7.292115856 \times 10^{-5}$ radians/seconds, the angular velocity of the earth. The conversion to the cartesian coordinates of the earth's rotating frame of reference (x_e, y_e, z_e) follows:

$$x_e = \cos(\rho) \times x + \sin(\rho) \times y$$

$$y_e = -\sin(\rho) \times x + \cos(\rho) \times y \tag{3.11}$$

$$z_e = z$$

To solve for the sub-satellite point of the satellite first convert the x_e, y_e, z_e coordinates to latitude, longitude and radius (ϕ, λ, r):

$$\phi = \sin^{-1}(z_e/\sqrt{(x_e^2 + y_e^2 + z_e^2)})$$

$$\lambda = \tan^{-1}(y_e/z_e) \qquad (3.12)$$

$$r = \sqrt{(x_e^2 + y_e^2 + z_e^2)}$$

Next, to compensate for the oblateness of the earth the following conversion is made to the latitude, longitude and radius of the sub-satellite point:

$$\phi_{sp} = \cos^{-1}(\cos(\phi)/\sqrt{(1-e_{earth}^2 \times \sin^{-2}(\phi))})$$

$$\lambda_{sp} = \lambda \qquad (3.13)$$

$$h_{sp} = r - R_{earth}(\phi)$$

where the radius of the earth, R, varies with latitude ϕ_{sp}. These values represent the location of a massless satellite orbiting a rotating, oblate earth.

For most applications modeling a satellite's position based on the two body Keplerian model (mass-less satellite and point mass earth) is not precise enough. Perturbations exist that cause the orbital elements of the satellite to vary. The particular elements that are affected depend upon the perturbing forces involved. Perturbations on the orbit of a satellite that cause no loss

in the total energy of the satellite (periodic perturbations) result in the values of a, e and i remaining virtually constant. The values for Ω, ω, and M, however, are affected. Examples of perturbing forces which cause little or no loss in the total energy of a satellite are the aspherical gravitational potential of the earth, the gravitational attraction of third bodies and radiation pressure from the sun.

Atmospheric drag can cause significant changes in the semi-major axis a, eccentricity and M, Ω, and ω depending on the operational altitude of the satellite under investigation. It is generally accepted that above heights of 850 kilometers the perturbing effects of the atmosphere (drag) becomes negligible. Since meteorological satellites operate at and above this level, the effects of drag induced perturbations are frequently ignored.

3. Asymmetrical Gravitational Potential

The model presented in Smith (1980) for use in determining the position of meteorological satellites considers only the asymmetrical gravitational potential of the earth and its effect on M, Ω, and ω. New values for the mean anomaly, longitude of the ascending node and argument of perigee are found by:

$$M = M_0 + \dot{M}(t - t_0)$$

$$\Omega = \Omega_0 + \dot{\Omega}(t - t_0) \qquad (3.13)$$

$$\omega = \omega_0 + \dot{\omega}(t - t_0)$$

where the first two approximations to the change in M, Ω, and ω, given in the order of increasing precision, are provided below:

(1st order approximation)

$$\dot{M} = \bar{n} = n[1 + 3/2\ J_2\ \frac{\sqrt{1-e^2}}{p^2}(1 - 3/2\ \sin^2(i)]$$

$$\dot{\Omega} = -(3/2\ J_2/p^2\ \cos(i))\bar{n} \qquad (3.15)$$

$$\dot{\omega} = -(3/2\ J_2/p^2\ (2 - 5/2\ \sin^2(i))\bar{n}$$

(2nd order approximation)

$$\dot{M} = \bar{n} = n[1 + 3/2\ J_2 \frac{\sqrt{1-e^2}}{p^2}\ (1 - 3/2\ \sin^2(i))$$

$$+ 3/128\ J_2{}^2 \frac{\sqrt{1-e^2}}{p^4}\ (16\ \sqrt{1 - e^2}$$

$$+ 25(1 - e^2) - 15 + 30 - 96(1 - e^2)^{1/2}$$

$$- 90(1 - e^2)\}\ \cos^2(i) + \{105 + 144(1 - e^2)^{1/2}$$

$$+ 25(1 - e^2)\}\ \cos^4(i)) - 45/128\ J_4(1 - e^2)^{1/2}/p^4$$

$$e^2(3 - 30\ \cos^2(i) + 35\ \cos^4(i))]$$

$$\dot{\Omega} = [3/2\ J_2/p^2\ \overline{n}\ \cos(i)(1 + 3/2\ J_2/p^2(3/2 + e^2/6 - 2(1 - e^2)^{1/2} - (5/3 - 5/24\ e^2 - 3(1 - e^2)^{1/2})\ \sin^2(i)))$$

$$+ 35/8\ J_4/p^4 n(1 + 3/2\ e^2)\ \frac{(12 - 21\ \sin^2(i))}{14}(\cos(i))] \qquad (3.16)$$

$$\dot{\omega} = [3/2\ J_2/p^2\ \overline{n}(2 - 5/2\ \sin^2(i))(1 + 3/2\ J_2/p^2 (2 + e^2/2 - 2(1 - e^2)^{1/2} - (43/24 - e^2/48 - 3(1 - e^2)^{1/2})\ \sin^2(i)))$$

$$- 45/36\ J_2/p^4\ e^2\ n\ \cos^4(i) - 35/8\ J_4/p^4\ n(12/7 - 93/14\ \sin^2(i) + 21/4\ \sin^4(i) + e^2(27/14 - 189/28\ \sin^2(i) + 81/16\ \sin^4(i)))]$$

where J_2 and J_4 are harmonic coefficients of the earth's asymmetrical gravitational potential approximated by (Smith, 1980):

$$J_2 = 1082.28 \times 10^{-6}$$

$$J_4 = -2.12 \times 10^{-6}$$

where P is the semi-parameter of an ellipse, $p = a(1 - e^2)$. Now the new values of Ω and ω must be found at time T since they are no longer constant:

$$\Omega_T = \Omega_0 + \dot{\Omega}(T - t_0)$$

$$\omega_T = \omega_0 + \dot{\omega}(T - t_0) \qquad (3.17)$$

with t_0 = epoch time and T - time of perifocal passage = $t_0 - M_0/n$. Finally, Ω and ω must be calculated at a specified time t:

$$\Omega = \Omega_T + \dot{\Omega}(t - T)$$
$$\omega = \omega_T + \dot{\omega}(t - T) \qquad (3.18)$$

These values are then substituted into the equations for x, y, and z, Equation (3.9), to account for the perturbing effect of the gravitational asymmetry of the earth. Upon completion of the above transformations, the satellite will be located in a rotating earth coordinate system.

The model illustrated above is a less sophisticated technique than the model being used at NPS since it does not consider any perturbing forces other than the asymmetrical gravitational potential of the earth. The next chapter will discuss the NPS model and how it addresses the other perturbative forces.

IV. NPS METHOD OF IMAGE NAVIGATION

A. DIGITAL DATA

The digital imagery data used for this investigation at the Naval Postgraduate School (NPS) is provided by the Scripps Institution of Oceanography. Digital imagery tapes provided by the Scripps Institution of Oceanography are referred to as HRPT (High Resolution Picture Transmission) tapes. These tapes consist of Advanced Very High Resolution Radiometer (AVHRR) images taken by the National Oceanic and Atmospheric Administration's (NOAA) polar orbiting satellites. It is on these images that the earth location of landmarks of interest must be resolved. In order to precisely locate a pixel on an image, the location of the imaging satellite within the image plane must be determined. Location of the satellite with respect to the image plane requires accurate location of both the satellite's ascending (or descending) node and its sub-satellite point. Before this can be accomplished, the satellite's position in an appropriate reference frame must be determined.

B. GEOCENTRIC REFERENCE FRAME

The information that describes the location of a satellite in the geocentric reference frame (a non-rotating earth reference frame) is called the ephemeris data. The ephemeris data on digital tapes acquired from the Navy Space

Surveillance System (NAVSPASUR) represent the orbital elements of the satellite at 0000Z Greenwich Mean Time (GMT). However, the majority of the imagery provided on the HRPT tapes is generated at a time T + 0000Z GMT. From the time 0000Z to T + 0000Z, the satellite has moved west relative to the earth in its orbit (approximately 15 degrees each hour). Therefore, the satellite's position (as represented by the ephemeris data) must be updated to time T. This is necessary to bring the satellite's position into agreement with the digital data provided on the HRPT tape.

Updating the satellite's position is accomplished through the use of an algorithm which is designed to take into consideration the time variance of the orbital elements as well as the perturbative effects of various forces acting on the satellite. Given the updated satellite position, the sub-satellite point can be determined. Although the ephemeris data provides an ascending node position, it may contain along track error due to the differences in time between the satellite's on board clock and the clock used to calibrate the ephemeris data. The satellite's ascending/ descending node is, therefore, calculated using the updated ephemeris data and known spherical geometry relationships.

Once the sub-satellite and the nodal points are calculated, the positions of the landmarks relative to the geocentric earth reference system can be found. The satellite imagery can then be "mapped" to the earth using

reference landmarks. The first step of this process is to develop models that accurately depict the satellite motion taking into consideration all relevant exogenous forces. The NPS method of determining the position of a satellite uses a series of subroutines that are called from the main (image navigation) program. Many of the relationships used in the subroutines are based on derivations developed by Smith (1980). These relationships were briefly outlined in Chapter III.

As discussed above, the major concern in locating a satellite is the process of updating its ephemeris data from epoch time to the time that is of interest to the user. For image navigation purposes, the time of interest is the time that the first line of the image was taken by the satellite's sensors. The subroutine that updates the orbital elements of the satellite is called AI_Calculate.

C. SUBROUTINE AI_CALCULATE

Subroutine AI_Calculate accesses (calls) four other subroutines; AIC_Elements, AIC_Semi-major, AIC_Perigee, and AIC_ASC_Node, to obtain the orbital elements of the satellite at epoch. Assuming that the eccentricity (e) and orbital inclination (i) are constant, AI_Calculate updates the remaining elements to the time corresponding to the time that the image was taken. It adjusts the semi-major axis (a), the argument of perigee (ω), the ascending node time, and the longitude of the ascending node (Ω) since these

values are time dependent. The ascending node location calculated in AIC_Asc_Node is not corrected for along track error, therefore, AIC_Asc_Node is not used. Instead, the position of the ascending node is calculated using an iterative/interactive routine called Twiddle. This procedure is explained following the descriptions of the subroutines that are used during navigation.

D. SUBROUTINE AIC_ELEMENTS

The first subroutine called by AI_Calculate is AIC_Elements. AIC_Elements reads the ephemeris data from the data files received from NAVSPASUR. The data read consists of: base anomaly (M_0, the mean anomaly (M) at epoch), mean motion (n), decay (time rate of change of the mean motion), eccentricity, perigee, longitude of the ascending node (Ω), inclination, record year, record month, and record day. Before accepting the data, the subroutine checks to ensure that the year and day of the data match the image being navigated.

The subroutine then converts the base anomaly, perigee, longitude of the ascending node, and the inclination to radians and saves them for use in other subroutines, e.g., AI_Calculate.

E. SUBROUTINE AIC_SEMI-MAJOR

The second subroutine accessed by the main subroutine, AI_Calculate, is the subroutine AIC_Semi-major.

AIC_Semi-major updates the semi-major axis (a), the mean motion constant (n) at epoch, and the mean anomaly (M). These updated values are necessary because of the perturbing effects of the asymmetrical gravitational potential (caused by the oblateness of the earth) on the satellite's orbit. To update the mean motion, the subroutine uses the relationship outlined by Smith (1980:94) that relates the mean motion at epoch, the earth's oblateness (represented by the second spherical harmonic, J_2), the orbital inclination, and the anomalistic period (p) to the anomalistic mean motion $\dot{M}$:

$$\dot{M} = \bar{n} = n[1 + 3/2\ J_2 \times \sqrt{(1 - e^2)}/p^2 \times (1 - 3/2\ \sin^2 i)] \ . \tag{4.1}$$

One refinement used in Subroutine AIC_Semi-major is the replacement of the anomalistic period (p) with an expression involving the semi-major axis (a):

$$p^2 = a^2(1 - e^2)^2 \tag{4.2}$$

Thus,

$$\dot{M} = \bar{n} = n[1 + 3/4\ J_2(3\ \cos^2 i - 1)/a^2(1 - e^2)^{3/2}] \tag{4.3}$$

This replacement enables the program to correct the mean motion and the semi-major axis length in an iterative process, ending when sufficient accuracy is obtained.

The mean anomaly is updated to account for the change in the mean motion, caused by the asymmetry of the earth's gravitational potential, using the following relationship:

$$M = M_0 + n \times t + \bar{n}t^2 \qquad (4.4)$$

where M_0 is the mean anomaly at epoch, n is the mean motion, $\bar{n}$ is the time rate of change of the mean motion, and t is the time since the orbital elements epoch time.

F. SUBROUTINE AIC_PERIGEE

The next subroutine accessed by AI_Calculate is the subroutine AIC_perigee, which calculates the argument of perigee for the satellite under consideration. AIC_Perigee solves for an updated argument of perigee by utilizing the relationship outlined by Smith (1980:94). The routine relates the updated argument of perigee (ω) to the argument of perigee at epoch (ω_0) plus the time rate of change of the argument of perigee ($\dot{\omega}$) due to the asymmetry of the earth:

$$\omega = \omega_0 + \dot{\omega}(t - t_0) \qquad (4.5)$$

where:

$$\dot{\omega} = (3/2\ J_2/p^2[2 - 5/2\ \sin^2 i])\bar{n} \ . \qquad (4.6)$$

As with AIC_Semi-major, Equation (4.6) is simplified by using the relationship between p and a (see Equation (4.2)).

G. TWIDDLE

Twiddle is a process that is used to determine the roll, pitch and yaw of the satellite and to calculate the ascending node position. The procedure is an iterative and interactive process that allows the user to "twiddle" (adjust) the assumed values of roll, pitch, and yaw and visualize the outcome of the adjustments. The effects of the twiddle process are illustrated by the amount of improvement in the total error figure. The total error figure represents the RMS differences between the positions of landmarks calculated during the navigation process, based on the assumed roll, pitch and yaw, and the charted values of the landmarks. Adjusting the roll, pitch or yaw can affect the total error by increasing the accuracy of the model that predicts the satellite's attitude. The main benefit of using the twiddle process is that it decreases the along track error leading to a better navigated image.

The known values used in the twiddle calculations are the landmark latitude (Lp) and the inclination of the satellite's orbit (i_= 180 - i). Roll, pitch, and yaw are assumed to be zero at the start and are modified during the interactive/iterative process.

The procedure illustrated below is based on the spherical geometry shown in Figures 5-8.

1. assume a value for roll, pitch, and yaw.

2. calculate $\gamma_{\_}$ from the sensor model:

$$\gamma_{\_} = \arctan[\sin(\text{angle} - \text{roll})/(\cos(\text{angle} - \text{roll})\sin(\text{pitch})] + \text{yaw} \quad (4.7)$$

= 90 degrees for 0 degree roll, pitch and yaw

where angle = mirror look angle (function of pixel #).

3. Calculate nadir angle (n):

$$n = \pi - \cos^{-1}[\cos(\text{angle} - \text{roll})\cos\text{pitch}] \quad (4.8)$$

$= \pi$ - angle, when roll, pitch and yaw = 0 degrees

4. From triangle I (Figure 6) calculate ϕ_g:

r = radius of earth at pixel (known)

h = height of satellite = r + average satellite height (average satellite height = 853 Km)

using the law of sines:

$$\sin(n)/r = \beta/h$$

$$\beta = h[\sin(n)/r] \quad (4.9)$$

knowing β and n:

$$\phi_g = 360 - (\beta + n) \quad (4.10)$$

we now know: ϕ_g, n, r, h, $\gamma_{\_}$, and LP.

5. The following relationships are used to calculate the longitude of the ascending node (λ_n):

$$\lambda_n = \lambda_p - \Delta\lambda_1 + \Delta\lambda_R \quad (4.11)$$

where λ_p is the known longitude of the landmark and $\Delta\lambda_R$ is an adjustment to the calculation for the longitude of the ascending node necessitated by the rotation of the earth. To account for the rotation, a time Δt is calculated using the orbital period (T_s):

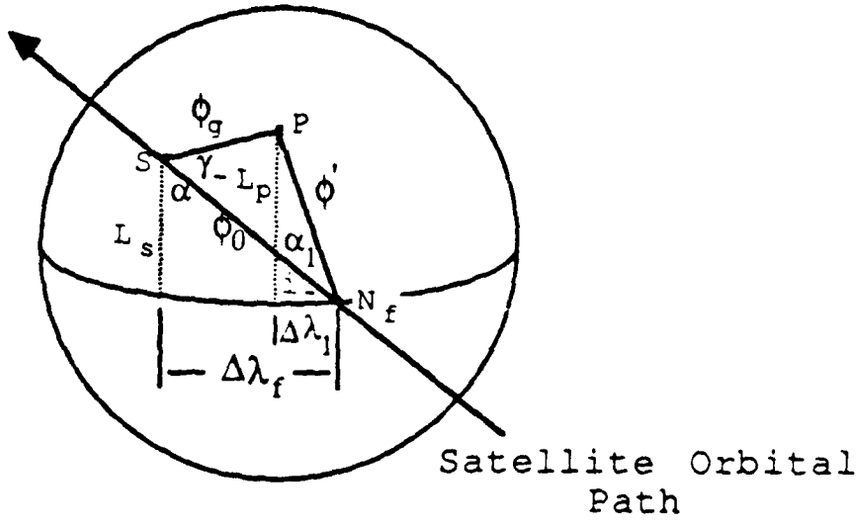

Figure 5. Satellite-Earth-Pixel Geometry

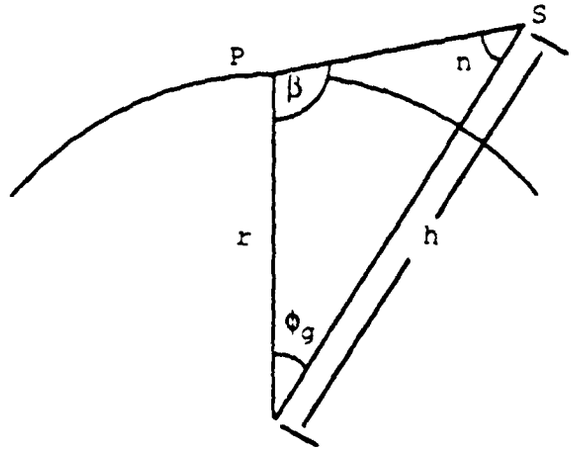

Figure 6. Earth-Satellite Geometry

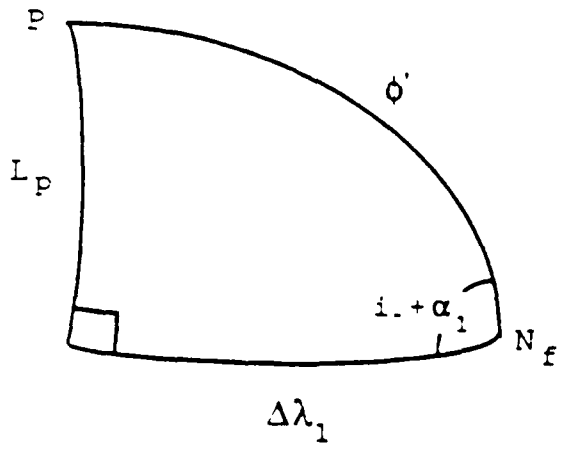

Figure 7. Spherical Triangle II

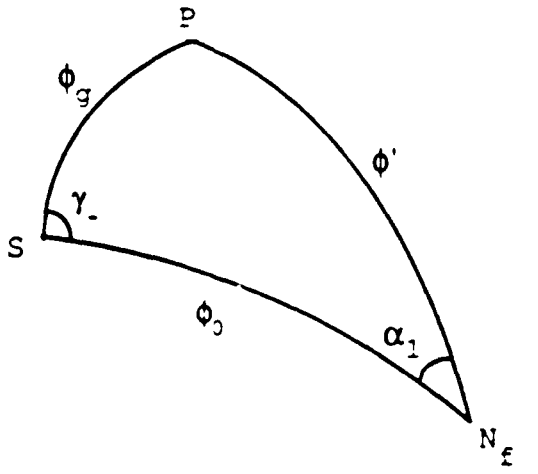

Figure 8. Spherical Triangle III

$$\Delta t = (T_s \times \phi_0)/2\pi \quad \text{so} \tag{4.12}$$

$$\Delta\lambda_R = [2\pi \times \Delta t/24 \times (1.002738)] \quad \text{(sidereal day adjustment)}$$

$$= 7.292117 \times 10^{-5} \text{ sec}^{-1} \times \Delta t \tag{4.13}$$

$\Delta\lambda_1$ is shown on triangle II (Figure 7):

$$\Delta\lambda_1 = \cos^{-1}[\cos\phi'/\cos LP] \tag{4.14}$$

where LP is the landmark latitude (known) and ϕ' must be determined.

6. To determine ϕ' the following calculations are made:

From triangle II (Figure 7):

$$\sin(i\_ + \alpha_1)/\sin LP = 1/\sin(\phi')$$
$$\sin(\phi') = \sin(LP)/\sin(i\_ + \alpha_1) \tag{4.15}$$

From triangle III (Figure 8):

$$\sin(\alpha_1)/\sin(\phi_g) = \sin(\gamma\_)/\sin(\phi') \tag{4.16}$$

Substituting in for $\sin(\phi')$:

$$\sin(\alpha_1)/\sin(\phi_g) = \sin(\gamma\_)\sin(i\_ + \alpha_1)/\sin(LP) \tag{4.17}$$

Isolating α_1:

$$\sin(LP)/\sin(\phi_g)\ \sin(\gamma\_) = \sin(i\_ + \alpha_1)/\sin(\alpha_1) \tag{4.18}$$

From trigonometry:

$$\sin(i\_ + \alpha_1) = \sin(\alpha_1)\ \cos(i\_) + \cos(\alpha_1)\ \sin(i\_) \tag{4.19}$$

Thus:

$$\sin(LP)/\sin(\phi_g)\ \sin(\gamma\_) = [\sin(\alpha_1)\ \cos(i\_) + \cos(\alpha_1)\ \sin(i\_)]/\sin(\alpha_1) \tag{4.20}$$

$$\sin(LP)/[\sin(\phi_g)\ \sin(\gamma\_)] = \cos(i\_) + \cot(\alpha_1)\ \sin(i\_) \tag{4.21}$$

$$\sin(LP)/[\sin(\phi_g)\ \sin(\gamma\_)] - \cos(i\_) = \cot(\alpha_1)\ \sin(i\_) \tag{4.22}$$

$$\cot(\alpha_1) = \sin(LP)/\sin(\phi_g)\ \sin(\gamma\_)\ \sin(i\_) - \cot(i\_) \quad (4.23)$$

so:

$$\alpha_1 = \cot^{-1}[\sin(LP)/\sin(\phi_g)\ \sin(\gamma\_)\ \sin(i\_) - \cot(i\_)] \quad (4.24)$$

(ϕ_g, α_1, $i\_$, and LP are all known)

From Equation (4.16):

$$\sin(\phi') = \sin(\gamma\_)\ \sin(\phi_g)/\sin(\alpha_1) \quad (4.25)$$

$$\phi' = \sin^{-1}[\sin(\gamma\_)\ \sin(\phi_g)/\sin(\alpha_1)] \quad (4.26)$$

With ϕ' calculated, the longitude of the ascending node can be determined using Equation (4.11).

As the user changes the roll, pitch, and yaw, the value for $\gamma\_$ and n (Equations (4.7) and (4.8)) change and the ascending node is recalculated. The "new" ascending node value is then used to recalculate positions of the landmarks and a RMS value is determined between the last calculated position and the new position. The error vectors used to portray the error of the assumed roll, pitch, and yaw are then based on the difference between the new positions and their respective RMS values. This process continues until the user is satisfied with the results represented by the total error.

Upon completion of the calculations performed in each of the above subroutines, the satellite is located within some degree of accuracy. The next step of the image navigation process is to determine the locations of the picture

elements (pixels) with respect to the satellite and earth geometry.

H. LOCATION OF PICTURE ELEMENTS

The NPS navigation program uses a series of functions to call subroutines that calculate pixel latitude, pixel longitude, satellite zenith and azimuth, and the solar zenith and azimuth. The processes performed by these subroutines and functions are called the forward navigation process. A summary of the major subroutines and the functions that comprise the forward package follows.

1. Subroutine AX_Check

Subroutine AX_Check is an intermediate subroutine that recovers the values for the pixel latitude, pixel longitude, the sub-satellite point, and the view vector from the satellite to the pixel. AX_Check calls either AX_Line_Values, AX_View_Vector, or AX_Pix_Latitude depending on where the pixel under consideration is located on the image plane.

a. AX_Line_Values

This subroutine is accessed when the scanner is not on the last line of the image plane. If the scanner is on the last line, this subroutine is skipped and AX_View_Vector is accessed. The subroutine AX_line_values determines the sub-satellite point of the satellite. The algorithms used in this subroutine require the knowledge of the scan line rate, the scan line number, the ascending node

time, the orbital period, and the orbital inclination. These are all values that have either been computed or have been gleaned from the ephemeris data file.

b. AX_View_Vector

The next subroutine called for by AX_Check is the AX_View_Vector subroutine. AX_View_Vector calculates the satellite's view vector for the pixel under consideration. The scanner mirror angle is calculated knowing the pixel number, then the view vector is resolved within the satellite coordinate system. The axes of this system are labeled x, y, and z. The x axis points in the opposite direction of the satellite orbit; the z axis points away from the earth; and the y axis completes a right hand cartesian coordinate system with the x and z axes.

c. AX_Pix_Latitude

AX_Check next calls the subroutine AX_Pix_ Latitude. The objective of this subroutine is to determine the pixel latitude in the geocentric-equatorial coordinate system. The subroutine accesses a series of other subroutines and functions to fulfill its role in the navigation process. Pixel latitude is resolved using the geometry between the scanner and the pixel, the known location of the sub-satellite point (S), and the known position of the nodal point (N_f)(see Figure 5).

d. AX_Pix_Longitude

Subroutine AX_Check next calls for the subroutine AX_Pixel_Longitude. AX_Pix_Longitude calculates the longitude of the requested pixel using many of the same known values that the subroutine AX_Pix_Latitude uses. The geometry of the problem is represented in Figure 5.

2. Function AX_Latitude

The function AX_Latitude is used to recover the value of the latitude of a pixel. In the process of retrieving the latitude of the pixel, the function calls the subroutine AX_Check. Subroutine AX_Check, as mentioned above, acts as an intermediary between the subroutines that calculate orbital and pixel elements and the function that utilizes them.

3. Function AX_Longitude

AX_Longitude recovers the longitude of a pixel. The pixel longitude is actually computed in the subroutine AX_Pix_Longitude and stored in the AX_Check subroutine. As a result, the function AX_Longitude must call the subroutine AX_Check to obtain the pixel longitude value.

The actual math used to compute the latitude, longitude, satellite zenith and all of the associated values needed to describe a pixel's location is straightforward and involves little complex calculations. The next section will describe the calculations based on the spherical triangles illustrated in Figure 8.

4. Forward Process

The process of generating the pixel locations (latitude and longitude) is called Forward. The location of individual pixels relative to the earth can be determined using spherical geometry and a knowledge of the relationships between the satellite and the earth, the scanner and the satellite, and the pixel and the scanner.

In the Forward process, the known quantities are the height of the satellite (h), the roll, pitch and yaw (as determined by the Twiddle process), and the orbital elements.

Values of $\alpha_{\_}$ and ϕ_g are calculated using Equations (4.7), (4.9), and (4.10) from the last section. The value of ϕ_0 is determined by dividing the time it takes the satellite to get to its position (from the ascending node) by the period of the satellite orbit. With these known values and the spherical geometry depicted in Figure 5, ϕ' and α_1 can be calculated as follows:

From the Law of Cosines and triangle III (Figure 8):

$$\cos(\phi') = \cos(\phi_g)\cos(\phi_0) + \sin(\phi_g)\sin(\phi_0)\cos(\gamma_{\_}) \tag{4.27}$$

$$\phi' = \cos^{-1}[\cos(\phi_g)\cos(\phi_0) + \sin(\phi_g)\sin(\phi_0)\cos(\gamma_{\_})]$$

Using Equation (4.16):

$$\sin(\alpha_1)/\sin(\phi_g) = \sin(\gamma_-)/\sin(\phi')$$
$$\sin(\alpha_1) = \sin(\phi_g)\ \sin(\gamma_-)/\sin(\phi') \qquad (4.28)$$
$$\alpha_1 = \sin^{-1}[\sin(\phi_g)\ \sin(\gamma_-)/\sin(\phi')]$$

Once α_1 and ϕ' are calculated, it is a simple matter to find the landmark latitude (LP):

Using Equation (4.15) and triangle II (Figure 7):

$$\sin(i_- + \alpha_1)/\sin(LP) = 1/\sin(\phi')$$
$$\sin(LP) = \sin(\phi')\ \sin(i_- + \alpha_1) \qquad (4.29)$$
$$LP = \sin^{-1}[\sin(\phi')\ \sin(i_- + \alpha_1)]$$

Now, knowing the longitude of the ascending node, calculated using:

$$\lambda_n = \lambda_p - \Delta\lambda_1 + \Delta\lambda_R \qquad (4.30)$$

The solution for the landmark longitude (λ_p) is:

$$\lambda_p = \lambda_n + \Delta\lambda_1 - \Delta\lambda_R \qquad (4.31)$$

where $\Delta\lambda_1$ is calculated using Equation (4.14) and $\Delta\lambda_R$ is calculated using Equation (4.13). The calculation of the landmark's position is therefore accomplished using

spherical geometry that accurately depicts the earth-satellite-pixel relationships in conjunction with constants calculated using the ephemeris data file from NAVSPASUR.

V. EXPERIMENTATION

A. STRATEGY OF LANDMARK SELECTION

In order to obtain a representation of the accuracy of the navigation program, a series of tests were developed. The tests consisted of the selection of various navigation landmark distributions. The different distributions were used to determine their influence on the image navigation accuracy. The navigation procedure begins with the user's selection of landmarks whose latitudes and longitudes are known (navigation landmarks). By identifying landmarks on the scene and in the geocentric earth reference system, and by applying a knowledge of the satellite's orbital elements, the satellite imagery is "mapped" to the earth using the method described in Chapter IV. When accomplished, any feature on the image should correspond exactly to its geographic location. The successful mapping of the image to the earth is called image registration.

There may exist, however, errors, in the image registration. These errors may be caused by inaccuracies in landmark identification or deviations from the predicted attitude or position of the satellite. To provide an estimate of the magnitude of the errors involved, a total error figure is reported during the navigation run.

The total error represents the root mean squared value of the differences between the calculated location of each

navigation landmark and its actual charted location. Since the total error is based on landmarks that are actually used in the navigation process itself, the true accuracy of the navigation process cannot be measured using the total error.

1. Accuracy Determination

A function provided in a subroutine of the NPS navigation program enables the navigation accuracy to be determined without using the total error. A series of test landmarks are selected from the satellite imagery and the computer calculates the latitudes and longitudes of the test landmarks based on the navigation that had already been accomplished. The computed locations are then compared with the actual charted latitudes and longitudes of the landmarks to obtain a measure of the accuracy of the navigation process.

2. Distribution of Landmarks

Attention should be focused on the image plane, not the image itself, for determination of the navigation landmark test distributions. Patterns of navigation landmarks should be selected based on their locations relative to the image plane, not necessarily with respect to the actual land-mass included in the image. Ideally, an unlimited number of navigation landmark distributions should be tested to obtain enough data to explore the effects of numerous landmark patterns on the accuracy of the navigation process. Important questions include:

1. What is the minimum amount of landmarks needed? e.g., zero, one, two....

2. What is the optimal layout of the landmarks? e.g., horizontally across the center of the image plane, horizontally across either the top or the bottom, vertically located in the center, vertically located on either side, or one landmark located in each corner of the image plane.

3. Is there a minimum distance beyond which two or more landmarks are necessary?

However, the ability to use varying distributions of navigation landmarks over the image plane is constrained by the amount of prominent features (usually water-land contrasts and landmass irregularities) that are available. For example, it may be desirable to test the effect of picking navigation landmarks that are located in the four corners of the image plane; however, this may be impossible to do if the only imagery available consists of a landmass that occupies only the bottom half of the image plane. To accommodate the imagery available and address the intuitive causative factors of error, the various distributions of navigation landmarks used are limited to a certain set. This set consists of navigation landmarks oriented parallel to the satellite's subtrack.

3. Distribution Choices

Since the majority of the imagery available to the NPS Department of Meteorology is of the U.S. West Coast, the distribution of landmarks is primarily constrained to the NW-SE direction. Although there exists imagery that may offer other distributions of landmarks, the amount of data

available is not enough to enable the production of significant results. Due to the imposed limitations, the effects of grouping landmarks parallel to the satellite subtrack (NW-SE) in several different regions of the image plane will be investigated.

There is some distortion associated with imagery along the edges of the image sensor's field of view because of the curvature of the earth. This distortion manifests itself as lower resolution imagery along the borders of the image plane. Landmarks picked close to the edges of the image plane can therefore be expected to result in larger navigation errors. Imagery that contains landmarks oriented parallel to and to the right and left hand sides of the satellite subtrack will be used to determine the influence of using landmarks obtained from areas of lower resolution. Imagery containing landmarks oriented along the satellite subtrack will also be navigated and tested. Landmarks oriented along the subtrack should have better resolution since the undesirable effects of being at the limbs of the scanner's field of view and of being in the area of the image plane, where the curvature of the earth is a factor, are minimized. The influence of various groupings of landmarks within the NW-SE columns will also be studied.

4. Procedural Experiment

A procedural experiment is set up as follows:

1. Categorize the images by their NW-SE distribution of landmarks as aligned left of subtrack, along subtrack (centered) or right of subtrack (Figures 9-11).

2. Perform the navigation for each category of images using the following procedures:

   a. Keeping the number of navigation landmarks constant: e.g., 2 or 4. This will test the effects of the displacement of the NW-SE landmark distributions (columns) from the satellite's subtrack. It will also determine the effects of using 2 versus 4 navigation landmarks (Figures 9-11).

   b. Vary the distance between 2 navigation landmarks from closely oriented (within 50 km) to far apart (greater than 500 km) (Figure 15).

   c. Using the centered distribution of landmarks, vary the along subtrack location of a group of 4 navigation landmarks. For example, 4 at the top, 4 at the bottom, or 4 in the center of the satellite subtrack (Figures 12-14).

   d. Using the centered distribution of landmarks, select 6 navigation landmarks equally spaced along the subtrack. Repeat the navigation adding one more navigation landmark close to one of the original 6 (Figure 16).

   e. Have a different person perform some of the image navigation runs.

3. Use the NPS navigation program's landmark location feature to quantify the effects of the various distributions mentioned above.

The amount of landmarks that are used to test the navigation process should be as numerous as possible and should also be randomly located within the image plane so as not to introduce any spurious effects from unnecessary patterns. The randomness of the testing landmarks is

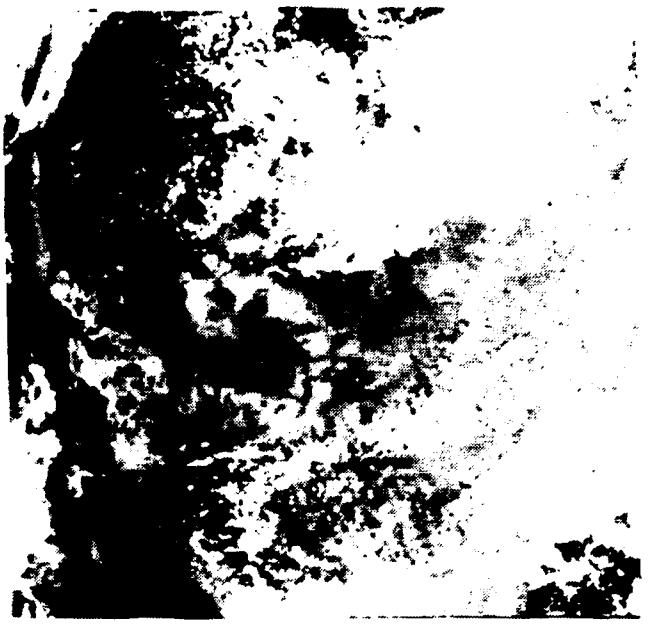

Figure 9. NOAA-9 Pass, 19 April 1986, 2139z, Displaying Imagery Oriented Left of Subtrack

Figure 10. NOAA-10 Pass, 17 September 1986, 2205z, Displaying Imagery Oriented Along Subtrack

Figure 11. NOAA-9 Pass, 20 April 1986, 2310z, Displaying Imagery Oriented Right of Subtrack

Figure 12. Same as Figure 10 with 4 Landmarks at Top of Imagery

Figure 13. Same as Figure 10 with 4 Landmarks Centered

Figure 14. Same as Figure 10 with 4 Landmarks at Bottom

Figure 15. Same as Figure 10 with 2 Landmarks Having Large Vertical Spread

Figure 16. Same as Figure 10 Adding 1 Landmark to 6 Equally Distributed Landmarks

constrained by the availability of imagery. The test landmarks used for the above experiment were located within the same NW-SE oriented columns as the navigation landmarks.

Using the described series of tests, the effects of the spatial distribution of navigation landmarks within columns parallel to the satellite subtrack are explored. The effects of the displacement of the parallel columns from the satellite subtrack are also examined. The results of these tests are summarized in Chapters VI and VII.

VI. RESULTS

A. EXPERIMENTAL RESULTS

The results from performing the registration of four different images in 22 separate cases are now summarized. Each case represents a distribution of navigation landmarks designed to test the effects of the distribution on registration accuracy. The distributions of navigation landmarks outlined in Chapter V are used. The number of navigation landmarks used varied from 2 to 16 depending on the particular distribution case under study.

1. Accuracy Measurement Methodology

The accuracy of the navigation was estimated by selecting test landmarks whose locations were computed by the NPS image registration program. These computed locations were compared to their actual charted locations to obtain a difference which is averaged for each image registered. The mean error is used as a gauge of the accuracy of the image registration process. A chord method that solves for the arc distance between two points was used to provide a meaningful measure of the differences between the computed and charted locations (Laurila, 1976:212-218). The algorithms take the latitude and longitude of two points (the computed and charted location of the test landmarks) and determine the arc distance between the points using

spherical geometry. The reference ellipsoid used in the chord method is the Department of Defense World Geodetic System 1984 (WGS-84) model ellipsoid. The WGS-84 is considered the best fitting reference ellipsoid used for mapping, charting, and geodesy.

Comparison of the chord method with more exact methods used on main frame computers indicate differences in computed distances of less than 6×10^{-8} at 1500 km and 10^{-6} at 10,000 km [Schnebele, 1988]. The accuracy of the chord method is dependent upon the precision of the computer or calculators used to implement it. The software used to calculate the arc distances between charted positions of landmarks and system generated positions is accurate to ±.005 km. This accuracy was considered more than adequate since the advertised resolution of the NOAA polar orbiter's sensors is 1.1 km.

2. Data Presentation

The data generated during the testing of the registration process, Table 1, represents a summary of the results obtained from the experimental procedure outlined in Chapter V. The runs listed are grouped by navigation landmark distribution. They are numbered to aid in the discussion of their significance. The number of landmarks column indicates both the number of navigation landmarks used in the initial image registration and the number of test landmarks used to determine the accuracy of the

TABLE 1

EXPERIMENTAL RESULTS

RUN #	TAPE #	#LANDMARKS NAV/TEST	DISPLACEMENT FROM SUBTRACK	VERTICAL DISTRIBUTION	MEAN ERROR
1	AR5290	02 12	LEFT	WIDE	4.54
2	AR5290	02 12	LEFT	VERY CLOSE-B	4.07
3	AR5290	02 12	LEFT	VERY CLOSE-K	4.24
4	17 SEP	02 12	ALONG TRACK	WIDE	2.75
5	17 SEP	02 12	ALONG TRACK	VERY CLOSE-B	2.93
6	17 SEP	02 12	ALONG TRACK	VERY CLOSE-K	2.31
7	AR5292	02 12	RIGHT	WIDE	3.82
8	AR5292	02 12	RIGHT	VERY CLOSE-B	2.73
9	AR5292	02 11	RIGHT	VERY CLOSE-K	2.95
10	AR6085	02 12	DIA. LFT.- RT.	WIDE	4.50
11	AR6085	02 12	DIA. LFT.- RT.	VERY CLOSE	4.68
12	17 SEP	04 12	ALONG TRACK	TOP	2.34
13	17 SEP	04 12	ALONG TRACK	BOTTOM-B	2.80
14	17 SEP	04 12	ALONG TRACK	BOTTOM-K	2.65
15	AR5290	04 12	LEFT	CENTER	4.95
16	17 SEP	04 12	ALONG TRACK	CENTER	2.41
17	AR5292	04 12	RIGHT	CENTER	3.10
18	17 SEP	06 17	ALONG TRACK	EVEN	1.77
19	17 SEP	07 17	ALONG TRACK	EVEN + 1	1.76
20	AR6085	16 32 / 18	DIA. LFT.- RT.	RANDOM	3.72 / 5.02
21	AR6085	13 32 / 23	DIA. LFT.- RT.	RANDOM	3.41 / 4.11
22	AR6085	16 33 / 19	DIA. LFT.- RT.	RANDOM	3.35 / 4.03
AVERAGE	--	05 15 / 14	-	--	3.26 / 3.38

registration. In runs 20-22 the mean error was calculated for test landmarks that included both the navigation landmarks and test landmarks. Therefore, there are two numbers listed under the test landmarks column. The first number is the number of test plus navigation landmarks used, the second number is the number of test landmarks only. It is important to note that the test landmarks used in each case were located within the same NW-SE column as the navigation landmarks. The displacement from subtrack column represents the displacement of each NW-SE oriented (West

Coast) column of landmarks from the satellite subtrack. For example, "along track" means the NW-SE column was located along the satellite subtrack (center of the image plane) (Figure 10, Chapter V). The vertical distribution column indicates where the navigation landmarks lie within each NW-SE column, irrespective of where the NW-SE column itself lies. These locations are dictated by the distribution scheme being tested. In the case where the image navigation and testing was repeated by another user, single letters B or K) appear at the end of the vertical distribution descriptors. These letters are the first letter of the last name of the user (Bethke or Kohrs). The mean error column lists the average arc distance between the system generated locations of test landmarks and the geographic locations of the test landmarks. These arc distances were calculated using the chord method referred to above and represent a measure of the accuracy of the NPS image registration process. In runs 20-22, the mean error was calculated twice. The first value represents the mean error based on test landmarks that include landmarks that were used as navigation landmarks. The second number is the mean error based on test landmarks comprised of landmarks other than the landmarks used for navigation.

B. ANALYSIS OF DATA TRENDS

Although there are not enough runs to produce statistically significant results, there are important

patterns that emerge from the analysis. These trends become obvious when the results are interpreted using operational experience on the image registration system. This section discusses the effects of various navigation landmark selection schemes on the accuracy of the image registration.

1. Effect of Initial Selection of Navigation Landmarks

One of the most important factors influencing the accuracy of the NPS image registration process is the accurate selection of navigation landmarks at the beginning of the registration process. Accurate selection of landmarks used to navigate the image is predicted by various factors. All of these factors are interrelated. The major constraints influencing the ability to choose "good" navigation landmarks include:

1. User's ability to discern "good" navigation landmarks: This constraint is subjective and includes such factors as the user's ability to see varying shades of gray. Since landmarks are frequently located on the coastline, the ability to recognize them is determined by the accurate choice of which particular pixel (the light gray one or the slightly darker gray one) represents the landmark. The ability to pick good landmarks is further affected by the quality of the imagery being registered.

2. Quality of Imagery: The quality of the imagery being registered is affected by various factors that include weather, geometry of the problem and geography. Cloudy weather obstructs landmarks decreasing the amount of available navigation landmarks. In situations where there are already a lack of navigation landmarks this result is undesirable. The sun-earth-satellite geometry may produce sunglint over the area that contains landmarks. Sunglint also prohibits the effective selection of good navigation landmarks. The quality of the imagery, for navigation purposes, is also affected by the geography of the land masses included in the imagery. Good

landmarks generally consist of geographical characteristics such as sharp land-water contrasts. Without the contrasts navigation landmarks become extremely difficult to select. The resolution of the imagery being registered is also a contributing factor in the ability or inability to select landmarks from areas of low contrasts.

3. Resolution: The resolution of the imagery is determined by the operational limitations of the satellite performing the imagery. The TIROS-N series of satellites have a nominal resolution of 1.1 km at nadir which constrains the ability to pick navigation landmarks which may be less than 1 km in area. It is important to note that the resolution is given as 1.1 km at nadir. Resolution decreases as the scan moves away from nadir off to either side. This decrease is caused by the curvature of the earth and the resultant angle between the sensor line of sight and the area being sensed. This decreasing resolution of oblique viewing is the motivating force behind studying the effects of the horizontal placement of the navigation landmark columns.

2. Effects of the Displacement from Subtrack of Landmark Columns

The displacement of navigation landmark columns from the satellite subtrack affects the resolution of the imagery being navigated. Landmarks oriented along the subtrack of the satellite are represented in the correct perspective since the surface being "mapped" is perpendicular to the line of sight (LOS) of the sensor. Navigation landmarks oriented to the right and left of the satellite's subtrack have a warped perspective since they are oblique to the LOS of the sensor (Figure 17). As a result, imagery consisting of land masses oriented to the far right or left of the image plane is distorted and presents difficulties in selecting navigation landmarks (see Figures 9 and 11, Chapter V).

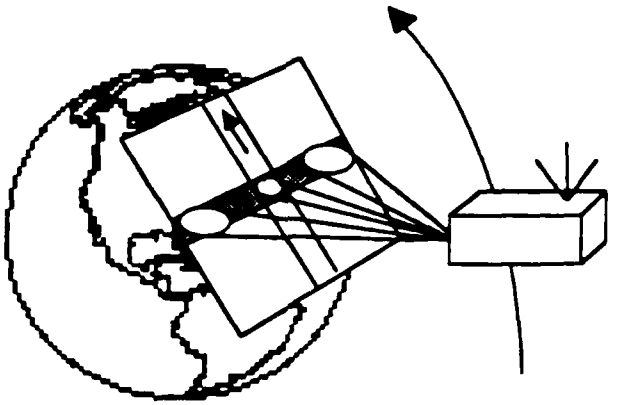

Figure 17. Scan Geometry of Satellite

In runs 1-19 the same navigation and test landmarks were used for each case under study. This was done to provide the best possible control and to isolate the case being studied, e.g., left oriented landmarks, from the spurious effects of using different landmarks from one run to the next. Runs 1-10 and 15-17 were performed to test the effects of the displacement of the navigation landmark columns from the subtrack (Table 1). Runs 1-3 and 15 consist of columns of landmarks oriented left of and parallel to the satellite subtrack. Since NOAA-9 Pass, 19 April 1986 (AR5290) contained imagery that was oriented to the far left side of the image plane, it was selected to use for these tests (Figure 9, Chapter V). Runs 4-6 and 16 were processed to study the effect of an along subtrack oriented

column of landmarks on the image registration accuracy. The tape used for this was 17 Sep 1987 since it offered imagery that was centrally oriented on the image plane (Figure 10, Chapter V). Runs 7-9 and 17 are NW-SE columns of landmarks oriented parallel and to the right of the subtrack. They were obtained from NOAA-9 Pass, 20 April 1986 (AR5292) (Figure 11, Chapter V) to test the influence that their distribution has on the image registration process.

Averaging the mean errors for the left, centered, and right oriented images (runs 1-10 and 16-18) resulted in values of 4.45 km, 2.60 km, and 3.15 km respectively. These results reinforce the concept that because of the curvature of the earth, landmarks oriented toward the left or right side of the image plane contribute to more error in the image registration than those centrally located. All of the runs studying the effects of the displacement of landmark columns from the subtrack had mean errors within the range of 2.31 km to 4.95 km.

3. Effects of the Distribution of Navigation Landmarks within NW-SE Columns

The effects of the distribution of navigation landmarks within each NW-SE column were explored in runs 1-19. Three cases were studied. The first case studied compared the effect that two widely separated navigation landmarks had on the navigation accuracy with the effect of two landmarks that were geographically close to one another (runs 1-11). The second case investigated the effects of

using 4 closely grouped navigation landmarks located at either the top, bottom, or center of the NW-SE column (runs 12-14 and 16). The third case studied the effect of 6 landmarks spaced evenly along the satellite subtrack.

It may be expected that two navigation landmarks with a wide vertical separation in the image would provide less mean error than two landmarks located close together. It seems intuitive that the widely separated navigation landmarks would provide a broader base than two closely located landmarks. The broader base would enable a better "fit" of the image to the earth. In runs 1-11, the effects of using two navigation landmarks only, either located close together or wide apart within a NW-SE column, are investigated. For runs 1, 4, and 7, the two navigation landmarks used to obtain a wide orientation were Punta Gorda in Northern California and Santa Cruz Island in Southern California. The two landmarks are approximately 818 km apart. For run 10, Needle Rocks point (off Pyramid Lake near the California-Nevada border), and Isle Angeles in the northern part of the Gulf of California are used. These navigation landmarks are about 1,614 km apart. Cape Mendocino and Punta Gorda, in Northern California, are used as the navigation landmarks for all of the closely oriented landmark cases (2-3, 5-6, 8-9, and 11). Their separation is approximately 20.3 km.

In order to provide a consistent basis for comparison, the wide and closely oriented cases are both investigated for the same NW-SE oriented landmark column, i.e., left of subtrack, centered (along subtrack), or right of subtrack. It would not be a valid approach to compare the effects of two widely separated navigation landmarks located in a NW-SE column on the left side of the image plane with two closely located navigation landmarks in a column on the right side. The comparison of cases within the same NW-SE oriented column shows the effects of the vertical separation (wide, close) of the navigation landmarks on the image registration for each column displaced from the subtrack. The effects of the vertical separation of the navigation landmarks for each displacement from subtrack (left, centered, and right) may then be compared to one another to explore any similarities in results.

Considering the case of landmarks oriented in a NW-SE column located parallel to and left of the subtrack (runs 1-3): the mean error for the widely spread (818 km) navigation landmarks (run 1) is 4.54 km, the errors for the closely held (20.3 km) navigation landmarks (runs 2 and 3) are 4.07 km and 4.24 km respectively.

In the case of navigation landmarks picked from a column located along the subtrack (runs 4-6), the mean errors for the two closely oriented (20.3 km) navigation

landmarks are 2.93 km and 2.31 km. For the widely separated case (818 km), the mean error is 2.75 km which falls between the errors of the closely oriented cases. For landmark columns located parallel to and to the right side of the subtrack (runs 7-9), the mean errors are 2.73 km and 2.95 km for the closely oriented case and 3.82 km for the widely separated navigation landmarks case. Runs 10 and 11 investigated the effects of varying the separation of two navigation landmarks that are diagonally oriented across the image plane from upper left to lower right. An effort was made to select navigation landmarks that were oriented vertically of one another. As stated above, Needle Rocks point and Isle Angeles were selected for the wide case (1,614 km apart) and Cape Mendocino and Punta Gorda were used for the closely oriented case (20.3 km). The results were a mean error of 4.50 km for the wide case and 4.68 km for the closely located case.

The differences in mean errors produced by the wide and close orientations of navigation landmarks for any of the four cases examined above are insignificant. A difference of less than 1 km for a system whose pixel resolution is only 1.1 km may be considered trivial. As illustrated, it is not justified to hypothesize that two widely separated navigation landmarks will yield a better image registration accuracy (smaller mean error) than two navigation landmarks located close together. In fact, the

averages of the mean errors for both the along track and right of subtrack cases are less for the two closely oriented navigation landmarks (2.62 km and 2.84 km respectfully) than the mean errors attributed to the widely separated navigation landmarks (2.75 km and 3.82 km).

A possible explanation for this behavior is that the mean errors for test landmarks selected in the vicinity of the navigation landmarks seems to be lower than the mean errors exhibited by test landmarks located further away. The hypothesis is that the low mean error associated with the test landmarks located around the two closely oriented navigation landmarks offsets the larger error associated with the test landmarks removed from the two navigation landmarks. The average is thus lower than for the widely dispersed navigation landmarks case which has larger mean errors associated with the test landmarks located around each of the single, widely separated navigation landmarks. Examination of run number 5 indicates an average mean error of 1.03 km for test landmarks located within 286 km of the two navigation landmarks compared to an average mean error of 4.47 km for test landmarks located at an average distance of 890 km from the two navigation landmarks. In run number 4, the average mean errors associated with test landmarks located near each of the single, widely separated navigation landmarks are 2.62 km and 3.41 km for the top and bottom navigation landmarks respectively.

In run 13, the navigation landmarks are located at the bottom of the image and test landmarks are grouped in locations 138 km, 582 km, and 977 km, from the navigation landmarks moving northward. Average mean errors associated with each of these groupings are 1.25 km, 3.92 km and 4.52 km respectively. These results support the observation that mean errors tend to increase for test landmarks located at distances farther from navigation landmarks and are representative of the general results for each case.

In runs 12-14 and 16, the effects of navigation landmarks located at the top, center and bottom of the landmark columns were explored. The results were difficult to interpret. It was expected that there would be no differences in the mean errors of these groups, but this was not observed. Performing the image registration using navigation landmarks situated near the top of the vertical columns (run 12), produced the smallest mean error of the three cases (2.34 km). Running the program using landmarks oriented toward the bottom (runs 13 and 14) seemed to contribute to the mean error (2.80 km, 2.65 km). It is important to note, however, that the differences in mean errors are small and may not be significant.

Runs 18 and 19 test the effects of using a NW-SE oriented, even distribution of landmarks on the image registration accuracy. Both of the runs utilized a NOAA-10 Pass, 17 September 1986, that offered navigation landmarks

along the subtrack of the satellite (Figure 10, Chapter V). Starting with Cape Flattery in Northern Washington State, a total of 6 navigation landmarks were picked with an average distance of 341 km between them. The landmarks extended down to Santa Cruz Island in Southern California. In run 19, an additional navigation landmark was selected (Punta Gorda) close to one of the 6 original navigation landmarks (within 20.3 km of Cape Mendocino). As shown in Table 1, the differences in mean errors (1.77 km and 1.76 km) are negligible. Runs 18 and 19 differed from the other runs utilizing tape number 17 Sep (runs 4-6, 12-14, and 16) because the navigation landmarks were as evenly spaced out as possible. The other runs used groups of landmarks at the top, center, or bottom of the imagery (runs 12-14 and 16), or two landmarks either widely separated or closely placed (runs 4-6). The evenly distributed cases (18 and 19) resulted in the lowest mean error out of all 22 runs performed (1.77 km and 1.76 km). This may be the result of enabling the navigation algorithms to fit more smoothly over the entire image vice over one specific area such as the bottom or top of the image plane.

4. Effects of Varying Numbers of Navigation Landmarks

Runs 20-22 were performed to examine the effects of picking as many navigation landmarks as possible. Out of a maximum number of 16 landmarks allowed by the system, two of the runs (20 and 22) used all of them and the other run (21)

used 13. The results of using the large number of landmarks were first tested using as many test landmarks as possible regardless of whether the same landmarks had been used as navigation landmarks. The mean errors generated by this scheme are 3.72 km, 3.41 km, and 3.35 km. Next, the results of using large numbers of navigation landmarks were tested using test landmarks other than the landmarks used as navigation landmarks. This produced mean errors of 5.02 km, 4.11 km, and 4.03 km. The lower mean errors from the first case are the direct result of using test landmarks that were also used as navigation landmarks. The important point to note is that the mean errors associated with randomly picking as many navigation landmarks as possible are not significantly better or worse in comparison to the other cases studied. For example, runs 1, 11, and 15 have mean errors of 4.54 km, 4.68 km and 4.95 km respectively (compare to 5.02 km, 4.11 km, and 4.03 km).

The examination of the differences in mean errors associated with using only two navigation landmarks vice four for the same horizontally located imagery yields interesting results. For example, comparing runs 1-3 (2 navigation landmarks) with run 15 (4 navigation landmarks) indicates errors of 4.54 km, 4.07 km and 4.24 km versus 4.95 km for left oriented imagery. Contrasting runs 4-6 (2 navigation landmarks) with 12-14 (4 navigation landmarks) shows mean errors of 2.75 km, 2.93 km and 2.31 km versus

2.34 km, 2.80 km and 2.65 km. These comparisons indicate that results obtained from using only 2 navigation landmarks can be as good as the results obtained from using four navigation landmarks.

The effects of different operators performing the image registration were documented for runs 2 and 3, 5 and 6, 8 and 9, and 13 and 14. The users had roughly the same operational familiarity with the image navigation process and the results bear this out. The mean errors for the comparison runs were 4.07 km and 4.24 km, 2.93 km and 2.31 km, 2.73 km and 2.95 km, and 2.80 km and 2.65 km respectively. This indicates that with the same training and operational exposure to the system, similar results can be expected from different users.

The final measure of the accuracy of the NPS image registration process is in the comparison of the average mean error of all 22 cases with the positioning errors reported in other sources. In the Clark and La Violette article cited in Chapter II, the mean positioning error for 32 landmark positions was given as 3.7 km (Clark, 1981:230). This average error was based on 4 registered TIROS-N images. The average mean error of the NPS method is 3.26 km/3.38 km. The two figures result from runs 20-22 where two cases were studied: test landmarks including landmarks that were used as navigation landmarks, and test landmarks without them.

VII. CONCLUSIONS/RECOMMENDATIONS

A. CONCLUSIONS

Based on the discussions included in the results section, the following conclusions may be made:

1. The ability of the user to accurately select both navigation and test landmarks is an overwhelming contributor to the accuracy of the navigation process. This ability is subjective and is affected by the quality of the imagery being registered.

2. The use of a large amount of navigation landmarks seems to constrain the registration problem to the point that differences in navigation landmark distributions are negligible. This seems to suggest that there may be a certain number of navigation landmarks after which adding any more doesn't appreciably add to the accuracy of the image registration.

3. Analysis of data trends suggest that navigation landmarks oriented towards the center of the image plane produce less mean error than navigation landmarks oriented to the left or right of the image plane.

4. Mean errors for test landmarks oriented close to the navigation landmarks are less than mean errors for test landmarks located further away from the navigation landmarks.

5. Navigation landmarks evenly distributed in a column along the subtrack tend to have smaller mean errors associated with them than navigation landmarks distributed either at the top, bottom, center, or randomly throughout a column oriented along the subtrack. The highest mean error for the evenly distributed case is 1.77 km, the lowest mean error of all the other cases is 2.31 km.

B. DIFFICULTIES/PROBLEMS ENCOUNTERED

The single most difficult obstacle to overcome is the learning curve that is associated with using the NPS image registration system. This learning curve manifests itself not only in the ability of the user to operate the system but in the ability of the user to accurately discern navigation and test landmarks. Learning which pixel represents the exact location of a landmark takes time and patience. For example, along the West Coast the pixels range from very light gray to dark gray depending on distance from land. The selection of the landmark becomes very subjective. Only after selecting and running the image registration process for each image and landmark within the image can the user get an idea as to which pixel is best.

Familiarity with the system and the commands/selections that are important will enable the user to register images more accurately and quickly. It is difficult to quantify the amount of time necessary to become proficient with the system since everyone's abilities are different. It took the author about three to four months to become comfortable with the system and confident in his abilities to accurately navigate imagery.

Since the operating system is continually being updated and newer, better ideas incorporated, keeping abreast of the changes and nuances caused by them is a continual effort.

C. RECOMMENDATIONS FOR FURTHER STUDY

The following list represents items that are a product of lessons learned by the author during the performance of the analysis of the accuracy of the NPS image registration system. The list is by no means an exhaustive list and may be improved upon with a little imagination and experience with the system.

1. Perform runs using various numbers of navigation landmarks but the same number of test landmarks for each run. This would help to determine the optimal (if there is one) number of navigation landmarks to use.

2. Perform more runs expanding on the results already obtained to provide a more statistically rigorous measure of the accuracy of the NPS image registration system.

3. Develop a method to separate user inaccuracies, i.e., the ability to select landmarks, from system inaccuracies to obtain a better (isolated) measure of the system inaccuracies. In an interactive system however, the user is part of the system. Perhaps it would be better to develop a system that eliminates or substantially decreases user involvement.

4. Develop a standardized training regimen for "image navigators." To include discussion on what makes a good landmark and the process of picking it off a map, determining the charted latitude and longitude, and entering it into the system. Hands on experience with selecting the correct pixels that make up the landmark under investigation should also be provided.

5. Look into the possibility/feasibility of developing an automatic landmark recognition process, perhaps using an expert system. At first cut, the system already knows approximately where the landmarks lie, perhaps a system can be developed that uses some sort of pixel-gray scale correlation scheme to precisely locate navigation landmarks.

6. Using the same imagery, navigation landmarks, and test landmarks, compare other system's ability to register the imagery with the NPS system's capabilities.

In general, there are many interacting forces at work when an image is navigated using an interactive system. Using the results contained in this thesis, one will be able to isolate more of the complex aspects of navigation thereby defining the contributions that each component makes to the accuracy of the NPS image registration process.

APPENDIX

GLOSSARY OF TERMS

Along track error--Difference between the actual position of a satellite along the projection of its orbit onto the ground and the computed location of the satellite within its projected orbit.

Anomalous motion--The motion of a satellite along its orbit caused by the action of perturbing forces.

Anomalistic Period--Time period between successive passes through the perifocus (point of closest approach to the primary), usually associated with perturbed orbits. The period does not remain constant (Taillefer, 1982).

Apogee--The point of furthest extent from the primary of a satellite within an elliptical orbit opposite the perigee along the major axis.

Argument of perigee (w)--Angle in the orbital plane from the ascending node to perigee (Smith, 1980).

Ascending node--Point where the satellite intersects the equatorial plane heading south to north.

Attitude--The orientation of a satellite with respect to a fixed reference system. Usually expressed in terms of roll, pitch, and yaw.

Computer compatible tape (CCT)--Magnetic data tapes on which digital imagery data is archived for future use.

Descending node--The point where a satellite intersects the equatorial plane heading north to south.

Digital imagery--A picture that has been transformed into an array of numbers for easy manipulation/transmission of the information contained within the picture.

Downlink--Transmission down to the earth (receiving station) of digital information from a satellite.

Eccentricity--The degree that a satellite's orbit varies from being circular (ellipticity).

Eccentric anomaly--An angle measured from the major axis to a line extended from the center of an ellipse to a point on a circumscribing circle whose position is determined by drawing a line from the satellite's position, perpendicular to the major axis, up to the circumscribing circle (see Figure 1).

Ecliptic--A great circle on the celestial sphere cut by the plane of the earth's orbit; the apparent annual path of the sun [Bader, 1962].

Ephemeris data--Information that describes the location of a satellite in its orbit at a specified time.

Epoch time--An arbitrarily picked time at which a set of orbital elements pertain.

Geostationary--An orbit around the equator whose period equals 24 hours giving the satellite the ability to remain fixed with respect to a point on the earth.

Ground Control Point (GCP)--Landmark selected from digital imagery, whose exact location is known, used in either image navigation or image rectification processes.

Ground Track--The Projection of a satellite's orbital track over the surface of the earth.

Image Navigation--A process involving the mapping of satellite imagery to the earth in an effort to establish a one to one correspondence between points on the earth and points in the imagery. Also called image registration.

Image Rectification--The correction of geometric distortion in an image. Usually performed by utilizing landmarks whose exact locations are known and who can be easily discerned within the digital imagery.

Image Registration--See image navigation.

Inclination (i)--The angle between the plane of the satellite's orbit and the equatorial plane of the earth [Smith, 1980].

Line of Nodes--The line connecting the ascending and descending nodes. Also called "nodal line" [Taillefer, 1982].

Mean Anomaly (m)--The angle through which a satellite would move in a time $t-t_o$, if traveling at a uniform average speed. Measured from perigee to the satellite with respect to the center of a mean circular orbit [Baker, et al., 1967:388].

Mean Circular Orbit--A circumscribing circle around a satellite's orbit that represents the orbit the satellite would travel in if it were moving at a uniform average speed.

Mean Motion (n)--Average angular speed of a satellite.

Major Axis--A line drawn through the center of an ellipse extending from perigee to apogee.

Nadir--A point on the earth described by the intersection of an imaginary plumb line, extended from a satellite, and the earth.

Navigation Landmarks--Landmarks selected from satellite digital imagery for use in the image navigation (registration) process.

Oblateness of the earth--A bulge in the earth located around the equator.

Orbital Elements--A set of numbers that describe the orbital characteristics of a satellite.

Orbital Plane--A plane defined by the orbit of a satellite.

Perigee--The point of closest approach to the earth of a satellite in an elliptical orbit.

Perturbative Force--An outside force acting on a satellite which causes anomalies in the satellite's orbit.

Real Time Imagery--Imagery that is collected by a satellite and downlinked to a receiving station without delay.

Right Ascension of Ascending Node (A)--Angle in the equatorial plane between the vernal equinox (reference meridian) and the northward equator crossing (ascending node) [Smith, 1980].

Satellite Zenith--The angle the satellite's velocity vector makes with the local vertical [Bate, et al., 1971].

Semi-Major Axis (a)--One half of the distance between perigee and apogee [Smith, 1980].

Semi-Minor Axis (b)--One half of the distance of a line passing through the center of an ellipse, drawn perpendicular to the semi-major axis.

Sidereal Hour Angle (SHA)--Angular distance west of the vernal equinox celestial meridian [Smith, 1980].

Sub-Satellite Point--See nadir point.

Sun Synchronous--An orbit that is such that the satellite maintains a constant geometry with the sun.

Test Landmarks--Landmarks selected from the digital imagery whose locations are known, used to test the accuracy of an image registration process.

Vernal Equinox--That point of intersection of the ecliptic and celestial equator where the sun crosses the equator from south to north in its apparent annual motion along the ecliptic [Baker, 1967].

LIST OF REFERENCES

Air Force Global Weather Central Report TM 74-1, The Scan Plane Method for Locating and Gridding Scanning Radiometer Satellite Data, by T.L. Cherne, January 1974.

Baker, R.M.L., and Makemson, M.W., An Introduction to Astrodynamics, 2d ed., Academic Press, 1967.

Bate, R.R., Mueller, D.D., and White, J.E., Fundamentals of Astrodynamics, Dover Publications Inc., 1971.

Brush, R.J.H., "A Method for Real-Time Navigation of AVHRR Imagery," IEEE Transactions on Geoscience and Remote Sensing, V. GE-23, No. 6, November 1985.

Clark, J.R. and LaViolette, P.E., "Detecting the Movement of Ocean Fronts Using Registered Tiros-N Imagery," Geophysical Research Letters, V. 8, No. 3, March 1981.

Department of Atmospheric Science, Colorado State University, Paper No. 321, Orbital Mechanics and Analytic Modelling of Meteorological Satellite Orbits, by E.A. Smith, February 1980.

El'yasberg, P.E., Introduction to the Theory of Flight of Artificial Earth Satellites, Israel Program for Scientific Translations, 1967.

European Space Agency, (esa sp-1011) Report N83-22018, A Glossary of Space Terms, by Y. Taillefer, November 1982.

Laurila, S.H., Electronic Surveying & Navigation, John Wiley & Sons, Inc., 1976.

Schnebele, K.J., GN3901 Mapping, Charting, and Geodesy, lab notes, presented at the Naval Postgraduate School, Monterey, California, 12 February 1988.

U.S. Department of Commerce, National Oceanic and Atmospheric Administration, National Environmental Satellite, Data and Information Service, National Climatic Data Center, Satellite Data Services Division, NOAA Polar Orbiter Data (TIROS-N, NOAA-6, NOAA-7, NOAA-8, NOAA-9, and NOAA-10) Users Guide, compiled by K.B. Kidwell, World Weather Building, Washington, D.C., December 1986.

BIBLIOGRAPHY

Barnea, D.I., "A Class of Algorithms for Fast Digital Image Registration," IEEE Transactions on Computers, V. C-21, No. 2, February 1972.

Caron, R.H. and Simon, K.W., "Attitude Time-Series Estimator for Rectification of Spaceborne Imagery," J. Spacecraft Rockets, V. 12, No. 1, January 1975.

Carton, D.S., Dynamics of Rockets and Satellites, North-Holland Publishing Company, 1965.

Environmental Science Services Administration, National Aeronautics and Space Administration, United States Air Force, U.S. Standard Atmospheric Supplements 1966, Government Printing Office, Washington, D.C., March 1981.

Escobal, P.R., Methods of Orbit Determination, John Wiley & Sons, Inc., 1965.

Ferns, D.C., "Microcomputer Systems for Satellite Image Processing," Earth-Orient. Applic. Space Technology, V. 4, 1984.

Hord, M.R., Remote Sensing, Methods and Applications, John Wiley & Sons, Inc., 1986.

Langdorf, K.A., Satellite Orbit Programs Utilizing the Graphics Capabilities of the Microcomputer, M.S. Thesis, Naval Postgraduate School, Monterey, California, June 1986.

Massey, H., Space Physics, Cambridge University Press, 1964.

National Aerospace Laboratory NLR, The Netherlands, report NLR MP 81039 U, On-Line Processing of High Resolution Imagery from Meteorological Satellites, by H.A. van Ingen Schenau, 7 July 1981.

National Aerospace Laboratory NLR, The Netherlands, report NLR-TR 82133 U, On-Line Superposition of Geographical Data to TIROS-N Type Meteorological Satellite Images, by R.G. van Popta, 23 December 1982.

Naval Research Laboratory, NRL Report 7975, Orbital Mechanics of General Coverage Satellites, by J.A. Eisele and S.A. Nichols, 30 April 1976.

Ng, K.Y.K., "An Automatic Image Registration and Overlay System," Computer and Electrical Engineering, V. 4, 1977.

Orth, R., Wong, F., and Macdonald, J.S., The Production of 1: 250,000 Maps of Precision Rectified and Registered LANDSAT Imagery Using the MDA Image Analysis System: Initial Results, paper presented at the International Symposium on Remote Sensing of Environment, 12th Proceeding, 1978.

Systems and Applied Sciences Corporation Report SAN-72, Formulation of a Unified Method for Earth Location and Gridding for Sun-Synchronous Satellites, by F.K. Chan, 15 March 1977.

INITIAL DISTRIBUTION LIST

		No. Copies
1.	Defense Technical Information Center Cameron Station Alexandria, Virginia 22304-6145	2
2.	Library, Code 0142 Naval Postgraduate School Monterey, California 93943-5000	2
3.	Prof. Rudolf Panholzer, Code 72 Chairman, Space Systems Academic Group Naval Postgraduate School Monterey, California 93943-5000	1
4.	LTC Linda K. Crumback, Code 39 Command, Control and Communications Naval Postgraduate School Monterey, California 93943-5000	1
5.	U.S. Space Command Attn: Technical Library Peterson AFB, Colorado 80914	1
6.	Commander Naval Space Command Dahlgren, Virginia 22448	1
7.	Office of the Chief of Naval Operations (OP-943) Department of the Navy Attn: CDR Nelson Spires Washington, D.C. 20350-2000	1
8.	Prof. Carlyle H. Wash, Code 63Wx Department of Meteorology Naval Postgraduate School Monterey, California 93943-5000	1
9.	Prof. Philip A. Durkee, Code 63De Department of Meteorology Naval Postgraduate School Monterey, California 93943-5000	1

10. Commander 1
Pacific Missile Test Center
Attn: Mr. Joseph P. Gannatal
Code 3152
Pt. Mugu, California 93042-5000

11. Capt. Kenneth L. Beutel 1
U.S. Space Command (J3SO) Stop 4
Peterson AFB, Colorado, 80914-5001

12. Capt. William J. Bethke 1
U.S. Space Command (J3SO) Stop 4
Peterson AFB, Colorado 80914-5001

END